44 Carlin, A. F. *et al.* An IRF-3-, IRF-5-, and IRF-7-Independent Pathway of Dengue Viral Resistance Utilizes IRF-1 to Stimulate Type I and II Interferon Responses. *Cell reports* **21**, 1600-1612, doi:10.1016/j.celrep.2017.10.054 (2017).
45 Chen, L. *et al.* Hepatic gene expression discriminates responders and nonresponders in treatment of chronic hepatitis C viral infection. *Gastroenterology* **128**, 1437-1444 (2005).
46 Randall, G. *et al.* Silencing of USP18 potentiates the antiviral activity of interferon against hepatitis C virus infection. *Gastroenterology* **131**, 1584-1591, doi:10.1053/j.gastro.2006.08.043 (2006).
47 Eroshkin, A. & Mushegian, A. Conserved transactivation domain shared by interferon regulatory factors and Smad morphogens. *J Mol Med (Berl)* **77**, 403-405 (1999).
48 Xu, P. *et al.* Innate antiviral host defense attenuates TGF-beta function through IRF3-mediated suppression of Smad signaling. *Mol Cell* **56**, 723-737, doi:10.1016/j.molcel.2014.11.027 (2014).

Supplementary References for methods

1 Brazil, D. P., Church, R. H., Surae, S., Godson, C. & Martin, F. BMP signalling: agony and antagony in the family. *Trends Cell Biol* **25**, 249-264, doi:10.1016/j.tcb.2014.12.004 (2015).
2 Cao, Y. & Zhang, L. A Smurf1 tale: function and regulation of an ubiquitin ligase in multiple cellular networks. *Cell Mol Life Sci* **70**, 2305-2317, doi:10.1007/s00018-012-1170-7 (2013).
3 Chen, D., Zhao, M. & Mundy, G. R. Bone morphogenetic proteins. *Growth Factors* **22**, 233-241, doi:10.1080/08977190412331279890 (2004).
4 Poorgholi Belverdi, M., Krause, C., Guzman, A. & Knaus, P. Comprehensive analysis of TGF-beta and BMP receptor interactomes. *Eur J Cell Biol* **91**, 287-293, doi:10.1016/j.ejcb.2011.05.004 (2012).
5 Core, A. B., Canali, S. & Babitt, J. L. Hemojuvelin and bone morphogenetic protein (BMP) signaling in iron homeostasis. *Front Pharmacol* **5**, 104, doi:10.3389/fphar.2014.00104 (2014).
6 Healey, E. G. *et al.* Repulsive guidance molecule is a structural bridge between neogenin and bone morphogenetic protein. *Nat Struct Mol Biol* **22**, 458-465, doi:10.1038/nsmb.3016 (2015).
7 Mueller, T. D. RGM co-receptors add complexity to BMP signaling. *Nat Struct Mol Biol* **22**, 439-440, doi:10.1038/nsmb.3037 (2015).
8 Besson-Fournier, C. *et al.* Induction of activin B by inflammatory stimuli up-regulates expression of the iron-regulatory peptide hepcidin through Smad1/5/8 signaling. *Blood* **120**, 431-439, doi:10.1182/blood-2012-02-411470 (2012).
9 Li, G., Heaton, J. H. & Gelehrter, T. D. Role of steroid receptor coactivators in glucocorticoid and transforming growth factor beta regulation of plasminogen activator inhibitor gene expression. *Mol Endocrinol* **20**, 1025-1034, doi:10.1210/me.2005-0145 (2006).
10 Seoane, J., Le, H. V., Shen, L., Anderson, S. A. & Massague, J. Integration of Smad and forkhead pathways in the control of neuroepithelial and glioblastoma cell proliferation. *Cell* **117**, 211-223 (2004).
11 Ge, D. *et al.* Genetic variation in IL28B predicts hepatitis C treatment-induced viral clearance. *Nature* **461**, 399-401 (2009).
12 Ikeda, M. *et al.* Efficient replication of a full-length hepatitis C virus genome, strain O, in cell culture, and development of a luciferase reporter system. *Biochemical and biophysical research communications* **329**, 1350-1359, doi:10.1016/j.bbrc.2005.02.138 (2005).
13 Hertzog, J. *et al.* Infection with a Brazilian isolate of Zika virus generates RIG-I stimulatory RNA and the viral NS5 protein blocks type I IFN induction and signaling. *European journal of immunology*, doi:10.1002/eji.201847483 (2018).
14 Rosenbloom, K. R. *et al.* ENCODE data in the UCSC Genome Browser: year 5 update. *Nucleic Acids Res* **41**, D56-63, doi:10.1093/nar/gks1172 (2013).

15 Trompouki, E. *et al.* Lineage regulators direct BMP and Wnt pathways to cell-specific programs during differentiation and regeneration. *Cell* **147**, 577-589, doi:10.1016/j.cell.2011.09.044 (2011).
16 Langmead, B. & Salzberg, S. L. Fast gapped-read alignment with Bowtie 2. *Nat Methods* **9**, 357-359, doi:10.1038/nmeth.1923 (2012).
17 Kent, W. J. *et al.* The human genome browser at UCSC. *Genome Res* **12**, 996-1006, doi:10.1101/gr.229102. Article published online before print in May 2002 (2002).
18 Heinz, S. *et al.* Simple combinations of lineage-determining transcription factors prime cis-regulatory elements required for macrophage and B cell identities. *Mol Cell* **38**, 576-589, doi:10.1016/j.molcel.2010.05.004 (2010).
19 McLean, C. Y. *et al.* GREAT improves functional interpretation of cis-regulatory regions. *Nat Biotechnol* **28**, 495-501, doi:10.1038/nbt.1630 (2010).
20 Verga Falzacappa, M. V., Casanovas, G., Hentze, M. W. & Muckenthaler, M. U. A bone morphogenetic protein (BMP)-responsive element in the hepcidin promoter controls HFE2-mediated hepatic hepcidin expression and its response to IL-6 in cultured cells. *Journal of molecular medicine* **86**, 531-540, doi:10.1007/s00109-008-0313-7 (2008).
21 Levy, D. E., Kessler, D. S., Pine, R., Reich, N. & Darnell, J. E., Jr. Interferon-induced nuclear factors that bind a shared promoter element correlate with positive and negative transcriptional control. *Genes & development* **2**, 383-393 (1988).
22 Parrington, J. *et al.* The interferon-stimulable response elements of two human genes detect overlapping sets of transcription factors. *European journal of biochemistry* **214**, 617-626 (1993).
23 Woodhouse, S. D. *et al.* Transcriptome sequencing, microarray, and proteomic analyses reveal cellular and metabolic impact of hepatitis C virus infection in vitro. *Hepatology* **52**, 443-453, doi:10.1002/hep.23733 (2010).
24 Sells, M. A., Chen, M. L. & Acs, G. Production of hepatitis B virus particles in Hep G2 cells transfected with cloned hepatitis B virus DNA. *Proc Natl Acad Sci U S A* **84**, 1005-1009 (1987).
25 Takahashi, I., Kobayashi, E., Asano, K., Yoshida, M. & Nakano, H. UCN-01, a selective inhibitor of protein kinase C from Streptomyces. *The Journal of antibiotics* **40**, 1782-1784 (1987).
26 Kawakami, K., Futami, H., Takahara, J. & Yamaguchi, K. UCN-01, 7-hydroxyl-staurosporine, inhibits kinase activity of cyclin-dependent kinases and reduces the phosphorylation of the retinoblastoma susceptibility gene product in A549 human lung cancer cell line. *Biochem Biophys Res Commun* **219**, 778-783, doi:10.1006/bbrc.1996.0310 (1996).
27 Akiyama, T. *et al.* G1 phase accumulation induced by UCN-01 is associated with dephosphorylation of Rb and CDK2 proteins as well as induction of CDK inhibitor p21/Cip1/WAF1/Sdi1 in p53-mutated human epidermoid carcinoma A431 cells. *Cancer research* **57**, 1495-1501 (1997).

Eddowes et al, Supplementary Information

Supplementary Tables and Table legends

	Controls N=8	SVR [b] N=17	NR [b] N=9
Age (yr). mean (95% CI)	67.4 (53.9 – 81.0), n=7[c]	36.8 (31.5 – 42.0), n=16 [c]	43.7 (37.3 – 50.1)
Sex (M/F)	8 / 0	9 / 8	4 / 5
Viral load (IU/mL), mean (95% CI)	-	1.06×10^6 (4.97×10^5 – 1.61×10^6), n=16 [c]	9.77×10^5 (4.67×10^4 – 1.91×10^6), n=8 [c]
HCV genotype (1 / 3)	-	11 / 6	7 / 2
Fibrosis stage (0 / mild / severe)[a]	-	10 / 7 / 0	3 / 6 / 0

Supplementary Table 1: Clinical parameters of control and HCV patients

[a] Fibrosis data is reported as follows: 0 = no fibrosis; mild = METAVIR 1-2 and Ishak 1-3; severe = METAVIR 3-4 and Ishak 4-6.
[b] Treatment outcome is reported as follows: SVR = HCV RNA negative 6 months post completion of therapy; NR = HCV RNA positive 6 months post therapy
[c] Missing patient information – data unavailable.

Extracellular ligands and inhibitors	BMP2, 4, 5, 6, 7, 9; Activin A, B, E; Noggin, Chordin, Follistatin
Cell surface receptors and co-receptor	ACVRL1, ACVR1, BMPR1A, BMPR1B ACVR2A, ACVR2B, BMPR2; HJV
Intracellular signal transduction factors, inhibitors, and key target genes	SMAD1, 4, 5, 6, 7, 8; SMURF1, 2, SKI, SKIL; EVI1; HAMP, ID1

Supplementary Table 2: BMP/Activin/hepcidin related signaling pathway components used for GWA enrichment analysis.

The general principles of BMP/SMAD signaling have been well explored and are the subject of ongoing study[1-4]. Here we focus on key BMP signaling components including those that have been shown to have *in vivo* effects on hepcidin regulation[5]. BMP ligands bind to the Type I BMP receptors BMPR1A (ALK3), BMPR1B (ALK6), ACVR1 (ALK2), and/or ACVRL1 (ALK1). Additionally, the BMP co-receptor HJV can recruit BMP2, BMP4, BMP5, BMP6 and BMP7 (but probably not BMP9)[6,7]. Noggin and chordin bind to BMPs and prevent them from binding to receptors. Activins A, B and E bind different type I receptors ACVR1B (ALK4) and ACVR1C (ALK7), although Activin B also utilizes BMP type I receptors in hepatocytes[8]. Activins are prevented from binding to their receptors by Follistatin.

After ligand binding, the ligand-receptor complexes (or ligand-HJV complexes) bind to the BMP type II receptors BMPR2, ACVR2A, and/or ACVR2B, (Activins only bind ACVR2A and ACVR2B) and the type II receptors phosphorylate type I receptors (which may displace HJV in endosomes). Activated BMP type I receptors BMPR1A, BMPR1B, ACVR1, and ACVR1L then bind and phosphorylate SMAD1, SMAD5 and SMAD8 (also known as SMAD9), together known as BMP R-SMADs. Activin type I receptors (ACVR1B and ACVR1C) bind and phosphorylate a different subset of R-SMAD proteins (SMAD2 and SMAD3), although Activin B can also signal through SMAD1, 5 or 8 in hepatocytes[8]. R-SMADs then bind to another SMAD, SMAD4. R-SMAD-SMAD4 complexes go to the nucleus and bind promoters of target genes, including SMAD6 and SMAD7. The encoded SMAD6 and SMAD7 proteins inhibit BMP signalling; SMAD6 binding targets include BMPR1B, inhibiting downstream phosphorylation of SMAD1 and SMAD5, while SMAD7 can bind to BMPR1A, BMPR1B and ACVR1, also inhibiting phosphorylation of SMAD1 and SMAD5. SMURF1 binds SMAD6 and SMAD7 and causes the ubiquitination and degradation of SMAD1, SMAD5, BMPR1B. SMURF2 can target SMAD1 for degradation. SKI, SKIL and EVI1 interact with SMAD1, SMAD5 and SMAD4 and repress BMP signalling. BMPs and Activin B induce expression of ID1 and HAMP in the liver.

Not included in the list are FOXG1 and GRIP1, which are not generally regarded as being part of the BMP signaling pathway; although both have been shown to regulate BMP signaling[9,10]. Several SNPs linked with FOXG1 and GRIP1 were also reported in the top 100 SNPs associated with differential HCV clearance [11]. Therefore there may be further significant enrichment of BMP-pathway variation associated with outcome of antiviral treatment of HCV.

ISG upregulated by BMP6	Effect of overexpression on HCV replication at 72h (see ref 21 of main ms)	ISG downregulated by BMP6	Effect of overexpression on HCV replication at 72h (see ref 21 of main ms)
JUNB	anti	ARG2	anti
IRF9	anti	GK	anti
LGALS3	anti	IL28RA	anti
HLA-E	anti	IMPA2	anti
ADM	anti	ZNF385B	anti
PSCD1	anti	IL1RN	anti
SSBP3	anti	THOC4	anti
PFKFB3	anti	GCH1	anti
LGMN	anti	PDGFRL	anti
CASP7	anti	USP18	anti
MAFB	anti	CCDC109B	anti
BLVRA	anti	VAMP5	anti
IFNGR1	anti	DUSP5	anti
TBX3	anti	C10orf10	anti
IFI6	anti	PUS1	pro
GLRX	anti	ETV6	pro
SOCS2	anti	CXCL10	pro
TMEM51	anti	CPT1A	pro
HK2	anti	IL17RB	pro
FAM125B	anti	ENPP1	pro
CCDC92	anti	MASTL	pro
ISG15	anti	RIPK2	pro
UBE2L6	anti	RNASE4	pro
SERPING1	anti	CD38	pro
TDRD7	anti	GPX2	pro
SPSB1	anti	FAM46A	pro
TRIM5	anti		
CDKN1A	anti		
HEG1	anti		
STAT2	anti		
IFI6	pro		
TXNIP	pro		
CD9	pro		
SP110	pro		
BCL3	pro		
AXUD1	pro		

Supplementary Table 3: Effect of BMP6 on expression of ISGs with known influence on HCV replication *in vitro.* We assessed the effect of BMP6 on expression of 355 known ISGs using our microarray of BMP6-treated HuH7.5 cells, in which 2275 genes were differentially expressed. The 355 ISGs chosen have been individually investigated for their effect on HCV replication in HuH7.5 cells (ref 21 of main ms, Schoggins et al Nature 2011). We found that BMP6 upregulated 36 of the 355 ISGs (30 of these 36 inhibited HCV replication in Schoggins et al 'anti') and downregulated 26 ISGs (14 of these 26 inhibited HCV replication in Schoggins et al).

Dataset	NCBI GEO Accession ID	ENCODE Accession ID	Cell type	Condition	Antibody
BMP4-SMAD1	GSM722416		K562	Human BMP4 @25ng/μL for 2h	SMAD1
IFNa6h-IRF1		wgEncodeEH001865	K562	Human IFNα; 6h	IRF1
Input control	GSM935363	wgEncodeEH000615	K562	Unstimulated	IgG
None-ARID3A	GSM935336	wgEncodeEH002861	K562	Unstimulated	ARID3A
None-ELK1		wgEncodeEH003356	K562	Unstimulated	ELK1
None-INI1	GSM935634	wgEncodeEH000725	K562	Unstimulated	INI1
None-RAD21	GSM935319	wgEncodeEH000649	K562	Unstimulated	RAD21
None-XRCC4	GSM935425	wgEncodeEH000650	K562	Unstimulated	XRCC4
Dorso-SMAD1	GSM722417		K562	Dorsomorphin @20 μM for 2h	SMAD1
IFNa6h-STAT1		wgEncodeEH000664	K562	Human IFNα; 6h	STAT1
IFNa6h-STAT2		wgEncodeEH000666	K562	Human IFNα; 6h	STAT2
None-RNA Pol II		wgEncodeEH000616	K562	Unstimulated	Pol2
None-RNA Pol III	GSM935481	wgEncodeEH000694	K562	Unstimulated	Pol3
CD34+ BMP4-SMAD1	GSM722399		CD34+	Human BMP4 @25ng/μL for 2h	SMAD1
U937 BMP4-SMAD1	GSM722425		U937	Human BMP4 @25ng/μL for 2h	SMAD1
CD34+ Input Control	GSM1097886		CD34+	Unstimulated	N/a
U937 Whole Cell Extract	GSM722431		U937	Unstimulated	N/a

Supplementary Table 4: ChIP-seq datasets interrogated in this study

GO BP: type I IFN-mediated signalling pathway	
Genes	**Genomic Regions of Peaks**
ADAR	chr1-2962 (-255635), chr1-1314 (-232445), chr1-5863 (-183715), chr1-1879 (-143724), chr1-3393 (-140074), chr1-4957 (-127712), chr1-2708 (-125585), chr1-5862 (-120979), chr1-554 (-112803), chr1-3607 (-111619), chr1-3092 (-106847), chr1-4956 (-17182), chr1-2825 (-15313), chr1-4036 (+33277)
EGR1	chr5-770 (-6920)
GBP2	chr1-4884 (-3979), chr1-3992 (-1115), chr1-5308 (-42)
HLA-A	chr6-2198 (-24431), chr6-336 (+22554), chr6-4512 (+39815)
HLA-C	chr6-2326 (+42784), chr6-849 (+55692), chr6-848 (+68097), chr6-2465 (+69094)
HLA-F	chr6-1069 (+11466), chr6-1772 (+39500), chr6-2948 (+40502)
HLA-G	chr6-2198 (+91060)
IFI35	chr17-502 (+7726), chr17-288 (+12451)
IFI6	chr1-698 (+9361), chr1-4186 (+13152)
IFIT1	chr10-694 (-7434), chr10-1229 (-104), chr10-1173 (+662)
IFIT2	chr10-3018 (-42885), chr10-404 (-6079), chr10-801 (-5415), chr10-830 (-443), chr10-1550 (+208), chr10-3019 (+24268)
IFIT3	chr10-3019 (-6265), chr10-1551 (-4537), chr10-693 (-4148), chr10-1718 (-64), chr10-1933 (+529), chr10-1279 (+1019), chr10-1124 (+14105)
IFNA1	chr9-953 (-28049), chr9-203 (+4001)
IFNA13	chr9-408 (-13802), chr9-2012 (+10100)
IFNA14	chr9-1830 (-55392), chr9-2181 (-55103), chr9-2413 (-47602), chr9-611 (-13485), chr9-2180 (-12475)
IFNA2	chr9-342 (-105), chr9-408 (+3519)
IFNA21	chr9-590 (+6282), chr9-818 (+13138)
IFNA5	chr9-1831 (-18046), chr9-1830 (+9942), chr9-2181 (+10231), chr9-2413 (+17732), chr9-611 (+51849), chr9-2180 (+52859)
IFNA6	chr9-2012 (-7089)
IFNA8	chr9-953 (+3258)
IFNAR1	chr21-896 (-86537), chr21-651 (-86118), chr21-455 (-82878), chr21-136 (-80679), chr21-343 (-79919), chr21-88 (-77092), chr21-173 (-64686), chr21-17 (-63130), chr21-180 (-59081), chr21-318 (-23775), chr21-373 (-23381), chr21-381 (-20104), chr21-181 (-15861), chr21-690 (-7671), chr21-344 (+37319), chr21-319 (+43371), chr21-802 (+49352), chr21-616 (+49639), chr21-63 (+55134), chr21-155 (+55806), chr21-306 (+58503), chr21-16 (+69524)
IFNAR2	chr21-217 (-150743), chr21-190 (-140306), chr21-688 (-133282), chr21-191 (-128529), chr21-154 (-120018), chr21-134 (-104800), chr21-275 (-101233), chr21-104 (-31015), chr21-475 (-26007), chr21-56 (-14144), chr21-290 (-13636), chr21-896 (+8446), chr21-651 (+8865), chr21-455 (+12105), chr21-136 (+14304), chr21-343 (+15064), chr21-88 (+17891), chr21-173 (+30297), chr21-17 (+31853), chr21-180 (+35902), chr21-318 (+71208), chr21-373 (+71602), chr21-381 (+74879), chr21-181 (+79122), chr21-690 (+87312)
IFNB1	chr9-784 (-41364), chr9-881 (-27009), chr9-1573 (-20031), chr9-842 (-19161), chr9-463 (-4245), chr9-988 (+16642), chr9-1684 (+30233)
IP6K2	chr3-2342 (-127879), chr3-3483 (-94900)
IRF1	chr5-2856 (-34641), chr5-2610 (-6287), chr5-2609 (-5116), chr5-1960 (+11297), chr5-545 (+22954), chr5-146 (+24117), chr5-461 (+33262), chr5-734 (+34144), chr5-2608 (+53010), chr5-1318 (+62891), chr5-70 (+64056), chr5-689 (+67890), chr5-639 (+69659), chr5-2607 (+75956), chr5-2385 (+100871), chr5-1851 (+102947)
IRF2	chr4-929 (-60206), chr4-550 (-39937), chr4-286 (-29648), chr4-1512 (-5256), chr4-1785 (-142), chr4-2439 (+13540), chr4-1318 (+20978), chr4-1027 (+22595), chr4-2154 (+56500), chr4-1388 (+78482), chr4-454 (+79576), chr4-810 (+90425), chr4-1952 (+91834), chr4-241 (+119227), chr4-928 (+127211), chr4-2153 (+128953), chr4-1511 (+160081), chr4-1951 (+180832), chr4-608 (+244268)

IRF4	chr6-753 (-94869), chr6-257 (-92958), chr6-1995 (-78550), chr6-792 (-54863), chr6-909 (-52064), chr6-344 (-50391), chr6-1370 (-19001), chr6-1171 (-7085), chr6-1093 (+31227), chr6-733 (+33605), chr6-1094 (+35070), chr6-1280 (+35405), chr6-3119 (+40552), chr6-2903 (+43050), chr6-2169 (+83260), chr6-1911 (+107431), chr6-2904 (+219305)
IRF5	chr7-1422 (-13764), chr7-2681 (-12976), chr7-608 (+2745), chr7-409 (+3314), chr7-64 (+10756), chr7-191 (+11197), chr7-1242 (+75618), chr7-549 (+76956)
IRF6	chr1-4097 (-2056), chr1-284 (+36621), chr1-1488 (+37715), chr1-1895 (+38255), chr1-3457 (+44989)
IRF7	chr11-2015 (-1071)
IRF8	chr16-2 (-69256), chr16-1902 (-60570), chr16-663 (-47490), chr16-43 (-45301), chr16-789 (-42945), chr16-2127 (-25847), chr16-1903 (-24928), chr16-1333 (-10194), chr16-313 (+6270), chr16-13 (+29458), chr16-486 (+37110), chr16-935 (+37415), chr16-218 (+44738), chr16-233 (+79109), chr16-50 (+83593), chr16-40 (+84591), chr16-301 (+85262), chr16-1906 (+97802), chr16-170 (+111845), chr16-688 (+115456), chr16-1242 (+118794), chr16-147 (+119570), chr16-1337 (+191041), chr16-790 (+270369), chr16-1107 (+314056), chr16-1568 (+408059), chr16-936 (+420984), chr16-664 (+442082), chr16-638 (+454231), chr16-1442 (+456832), chr16-260 (+480400), chr16-1338 (+516377), chr16-566 (+549124), chr16-882 (+549527)
ISG20	chr15-2334 (-16253), chr15-2862 (-15528), chr15-931 (-59)
JAK1	chr1-370 (-130792), chr1-1606 (-89499), chr1-5736 (-88169), chr1-4868 (+9703), chr1-5287 (+32060), chr1-3362 (+33046), chr1-4239 (+49056), chr1-4867 (+68281), chr1-1995 (+70830), chr1-1866 (+102235), chr1-7092 (+220013)
MX1	chr21-219 (-29419), chr21-261 (-5780)
MX2	chr21-370 (+14), chr21-219 (+34609), chr21-261 (+58248)
OAS1	chr12-3290 (-50853), chr12-795 (-36159), chr12-250 (-19252), chr12-3693 (-13867), chr12-764 (-57), chr12-1227 (+603)
OAS2	chr12-2145 (-38339), chr12-928 (-64), chr12-1121 (+62301)
OAS3	chr12-2145 (+1686)
OASL	chr12-3010 (-71387), chr12-931 (-57537), chr12-1124 (-56690), chr12-735 (-53984), chr12-3317 (-48933), chr12-1231 (-10627), chr12-2736 (+2168), chr12-1176 (+4879)
PSMB8	chr6-543 (-1622), chr6-2470 (-1186)
PTPN1	chr20-35 (-288668), chr20-1004 (-249610), chr20-480 (-239621), chr20-110 (-238049), chr20-312 (-235277), chr20-548 (-226294), chr20-245 (-212650), chr20-209 (-207799), chr20-246 (-171500), chr20-654 (-163639), chr20-189 (-162120), chr20-101 (-160896), chr20-257 (-156696), chr20-1254 (-143608), chr20-584 (-138063), chr20-76 (-130955), chr20-1087 (-128016), chr20-1324 (-124192), chr20-2181 (-106582), chr20-247 (-100603), chr20-508 (-97107), chr20-328 (-75497), chr20-786 (-69721), chr20-496 (-69325), chr20-463 (-59340), chr20-105 (-54370), chr20-1191 (-52322), chr20-787 (+6445), chr20-481 (+7600), chr20-58 (+31467), chr20-1192 (+62830), chr20-1632 (+126717), chr20-1193 (+130618), chr20-266 (+142443), chr20-443 (+200475)
PTPN11	chr12-1782 (+28612), chr12-1226 (+163632), chr12-794 (+181381)
PTPN6	chr12-3057 (-3014), chr12-2329 (-2608), chr12-1135 (+4704), chr12-536 (+7409), chr12-1915 (+12303), chr12-347 (+12665), chr12-2330 (+15293)
RNASEL	chr1-1955 (+48911), chr1-6620 (+68398), chr1-67 (+104425), chr1-512 (+128556), chr1-1775 (+129068)
SOCS1	chr16-1602 (-9533), chr16-1122 (-8276), chr16-642 (+19017), chr16-999 (+21978), chr16-455 (+22959), chr16-454 (+36801), chr16-641 (+47142), chr16-593 (+49998), chr16-469 (+54091), chr16-1057 (+74068), chr16-1951 (+110583), chr16-1950 (+117312), chr16-1266 (+119379), chr16-570 (+120608), chr16-1180 (+127211), chr16-1056 (+129345), chr16-1756 (+131751), chr16-468 (+151066), chr16-354 (+161741), chr16-998 (+162078), chr16-362 (+173235), chr16-291 (+176443), chr16-1265 (+189563), chr16-70 (+203644), chr16-668 (+205101), chr16-890 (+207296), chr16-1755 (+221342), chr16-547 (+221972), chr16-1357 (+260483), chr16-1055 (+306607), chr16-438 (+322882), chr16-799 (+370750), chr16-723 (+374370)
SOCS3	chr17-826 (+16249), chr17-1223 (+22384), chr17-51 (+30513), chr17-525 (+35276), chr17-1950 (+65135), chr17-2529 (+65997), chr17-2119 (+66730), chr17-2756 (+67237), chr17-1827 (+74770), chr17-2118 (+75749)
SP100	chr2-2369 (-3570), chr2-1251 (+19), chr2-4992 (+2390), chr2-4993 (+23702), chr2-190 (+41431), chr2-6135 (+162016), chr2-3944 (+173551), chr2-475 (+227527), chr2-1817 (+227979), chr2-319 (+244660), chr2-1121 (+252511), chr2-4996 (+253022), chr2-4193

	(+262424), chr2-2680 (+284442)
STAT1	chr2-3280 (-100570), chr2-4931 (-37861), chr2-4508 (-24304), chr2-3911 (-6895), chr2-1929 (+17051), chr2-841 (+43193), chr2-2932 (+52159), chr2-3279 (+66201), chr2-3910 (+122614)
STAT2	chr12-2875 (+1157)
TYK2	chr19-577 (+7643)
USP18	chr22-9 (-35843), chr22-503 (-30016)
XAF1	chr17-341 (-3177), chr17-774 (-2667), chr17-3083 (+40776)

GO BP: response to type I IFN	
Genes	**Genomic Regions of Peaks**
ADAR	chr1-2962 (-255635), chr1-1314 (-232445), chr1-5863 (-183715), chr1-1879 (-143724), chr1-3393 (-140074), chr1-4957 (-127712), chr1-2708 (-125585), chr1-5862 (-120979), chr1-554 (-112803), chr1-3607 (-111619), chr1-3092 (-106847), chr1-4956 (-17182), chr1-2825 (-15313), chr1-4036 (+33277)
EGR1	chr5-770 (-6920)
GBP2	chr1-4884 (-3979), chr1-3992 (-1115), chr1-5308 (-42)
HLA-A	chr6-2198 (-24431), chr6-336 (+22554), chr6-4512 (+39815)
HLA-C	chr6-2326 (+42784), chr6-849 (+55692), chr6-848 (+68097), chr6-2465 (+69094)
HLA-F	chr6-1069 (+11466), chr6-1772 (+39500), chr6-2948 (+40502)
HLA-G	chr6-2198 (+91060)
IFI35	chr17-502 (+7726), chr17-288 (+12451)
IFI6	chr1-698 (+9361), chr1-4186 (+13152)
IFIT1	chr10-694 (-7434), chr10-1229 (-104), chr10-1173 (+662)
IFIT2	chr10-3018 (-42885), chr10-404 (-6079), chr10-801 (-5415), chr10-830 (-443), chr10-1550 (+208), chr10-3019 (+24268)
IFIT3	chr10-3019 (-6265), chr10-1551 (-4537), chr10-693 (-4148), chr10-1718 (-64), chr10-1933 (+529), chr10-1279 (+1019), chr10-1124 (+14105)
IFNA1	chr9-953 (-28049), chr9-203 (+4001)
IFNA13	chr9-408 (-13802), chr9-2012 (+10100)
IFNA14	chr9-1830 (-55392), chr9-2181 (-55103), chr9-2413 (-47602), chr9-611 (-13485), chr9-2180 (-12475)
IFNA2	chr9-342 (-105), chr9-408 (+3519)
IFNA21	chr9-590 (+6282), chr9-818 (+13138)
IFNA5	chr9-1831 (-18046), chr9-1830 (+9942), chr9-2181 (+10231), chr9-2413 (+17732), chr9-611 (+51849), chr9-2180 (+52859)
IFNA6	chr9-2012 (-7089)
IFNA8	chr9-953 (+3258)
IFNAR1	chr21-896 (-86537), chr21-651 (-86118), chr21-455 (-82878), chr21-136 (-80679), chr21-343 (-79919), chr21-88 (-77092), chr21-173 (-64686), chr21-17 (-63130), chr21-180 (-59081), chr21-318 (-23775), chr21-373 (-23381), chr21-381 (-20104), chr21-181 (-15861), chr21-690 (-7671), chr21-344 (+37319), chr21-319 (+43371), chr21-802 (+49352), chr21-616 (+49639), chr21-63 (+55134), chr21-155 (+55806), chr21-306 (+58503), chr21-16 (+69524)
IFNAR2	chr21-217 (-150743), chr21-190 (-140306), chr21-688 (-133282), chr21-191 (-128529), chr21-154 (-120018), chr21-134 (-104800), chr21-275 (-101233), chr21-104 (-31015), chr21-475 (-26007), chr21-56 (-14144), chr21-290 (-13636), chr21-896 (+8446), chr21-651 (+8865), chr21-455 (+12105), chr21-136 (+14304), chr21-343 (+15064), chr21-88 (+17891), chr21-173 (+30297), chr21-17 (+31853), chr21-180 (+35902), chr21-318 (+71208), chr21-373 (+71602), chr21-381 (+74879), chr21-181 (+79122), chr21-690 (+87312)

IFNB1	chr9-784 (-41364), chr9-881 (-27009), chr9-1573 (-20031), chr9-842 (-19161), chr9-463 (-4245), chr9-988 (+16642), chr9-1684 (+30233)
IP6K2	chr3-2342 (-127879), chr3-3483 (-94900)
IRF1	chr5-2856 (-34641), chr5-2610 (-6287), chr5-2609 (-5116), chr5-1960 (+11297), chr5-545 (+22954), chr5-146 (+24117), chr5-461 (+33262), chr5-734 (+34144), chr5-2608 (+53010), chr5-1318 (+62891), chr5-70 (+64056), chr5-689 (+67890), chr5-639 (+69659), chr5-2607 (+75956), chr5-2385 (+100871), chr5-1851 (+102947)
IRF2	chr4-929 (-60206), chr4-550 (-39937), chr4-286 (-29648), chr4-1512 (-5256), chr4-1785 (-142), chr4-2439 (+13540), chr4-1318 (+20978), chr4-1027 (+22595), chr4-2154 (+56500), chr4-1388 (+78482), chr4-454 (+79576), chr4-810 (+90425), chr4-1952 (+91834), chr4-241 (+119227), chr4-928 (+127211), chr4-2153 (+128953), chr4-1511 (+160081), chr4-1951 (+180832), chr4-608 (+244268)
IRF4	chr6-753 (-94869), chr6-257 (-92958), chr6-1995 (-78550), chr6-792 (-54863), chr6-909 (-52064), chr6-344 (-50391), chr6-1370 (-19001), chr6-1171 (-7085), chr6-1093 (+31227), chr6-733 (+33605), chr6-1094 (+35070), chr6-1280 (+35405), chr6-3119 (+40552), chr6-2903 (+43050), chr6-2169 (+83260), chr6-1911 (+107431), chr6-2904 (+219305)
IRF5	chr7-1422 (-13764), chr7-2681 (-12976), chr7-608 (+2745), chr7-409 (+3314), chr7-64 (+10756), chr7-191 (+11197), chr7-1242 (+75618), chr7-549 (+76956)
IRF6	chr1-4097 (-2056), chr1-284 (+36621), chr1-1488 (+37715), chr1-1895 (+38255), chr1-3457 (+44989)
IRF7	chr11-2015 (-1071)
IRF8	chr16-2 (-69256), chr16-1902 (-60570), chr16-663 (-47490), chr16-43 (-45301), chr16-789 (-42945), chr16-2127 (-25847), chr16-1903 (-24928), chr16-1333 (-10194), chr16-313 (+6270), chr16-13 (+29458), chr16-486 (+37110), chr16-935 (+37415), chr16-218 (+44738), chr16-233 (+79109), chr16-50 (+83593), chr16-40 (+84591), chr16-301 (+85262), chr16-1906 (+97802), chr16-170 (+111845), chr16-688 (+115456), chr16-1242 (+118794), chr16-147 (+119570), chr16-1337 (+191041), chr16-790 (+270369), chr16-1107 (+314056), chr16-1568 (+408059), chr16-936 (+420984), chr16-664 (+442082), chr16-638 (+454231), chr16-1442 (+456832), chr16-260 (+480400), chr16-1338 (+516377), chr16-566 (+549124), chr16-882 (+549527)
ISG20	chr15-2334 (-16253), chr15-2862 (-15528), chr15-931 (-59)
JAK1	chr1-370 (-130792), chr1-1606 (-89499), chr1-5736 (-88169), chr1-4868 (+9703), chr1-5287 (+32060), chr1-3362 (+33046), chr1-4239 (+49056), chr1-4867 (+68281), chr1-1995 (+70830), chr1-1866 (+102235), chr1-7092 (+220013)
MX1	chr21-219 (-29419), chr21-261 (-5780)
MX2	chr21-370 (+14), chr21-219 (+34609), chr21-261 (+58248)
OAS1	chr12-3290 (-50853), chr12-795 (-36159), chr12-250 (-19252), chr12-3693 (-13867), chr12-764 (-57), chr12-1227 (+603)
OAS2	chr12-2145 (-38339), chr12-928 (-64), chr12-1121 (+62301)
OAS3	chr12-2145 (+1686)
OASL	chr12-3010 (-71387), chr12-931 (-57537), chr12-1124 (-56690), chr12-735 (-53984), chr12-3317 (-48933), chr12-1231 (-10627), chr12-2736 (+2168), chr12-1176 (+4879)
PSMB8	chr6-543 (-1622), chr6-2470 (-1186)
PTPN1	chr20-35 (-288668), chr20-1004 (-249610), chr20-480 (-239621), chr20-110 (-238049), chr20-312 (-235277), chr20-548 (-226294), chr20-245 (-212650), chr20-209 (-207799), chr20-246 (-171500), chr20-654 (-163639), chr20-189 (-162120), chr20-101 (-160896), chr20-257 (-156696), chr20-1254 (-143608), chr20-584 (-138063), chr20-76 (-130955), chr20-1087 (-128016), chr20-1324 (-124192), chr20-2181 (-106582), chr20-247 (-100603), chr20-508 (-97107), chr20-328 (-75497), chr20-786 (-69721), chr20-496 (-69325), chr20-463 (-59340), chr20-105 (-54370), chr20-1191 (-52322), chr20-787 (+6445), chr20-481 (+7600), chr20-58 (+31467), chr20-1192 (+62830), chr20-1632 (+126717), chr20-1193 (+130618), chr20-266 (+142443), chr20-443 (+200475)
PTPN11	chr12-1782 (+28612), chr12-1226 (+163632), chr12-794 (+181381)
PTPN6	chr12-3057 (-3014), chr12-2329 (-2608), chr12-1135 (+4704), chr12-536 (+7409), chr12-1915 (+12303), chr12-347 (+12665), chr12-2330 (+15293)
RNASEL	chr1-1955 (+48911), chr1-6620 (+68398), chr1-67 (+104425), chr1-512 (+128556), chr1-1775 (+129068)

SOCS1	chr16-1602 (-9533), chr16-1122 (-8276), chr16-642 (+19017), chr16-999 (+21978), chr16-455 (+22959), chr16-454 (+36801), chr16-641 (+47142), chr16-593 (+49998), chr16-469 (+54091), chr16-1057 (+74068), chr16-1951 (+110583), chr16-1950 (+117312), chr16-1266 (+119379), chr16-570 (+120608), chr16-1180 (+127211), chr16-1056 (+129345), chr16-1756 (+131751), chr16-468 (+151066), chr16-354 (+161741), chr16-998 (+162078), chr16-362 (+173235), chr16-291 (+176443), chr16-1265 (+189563), chr16-70 (+203644), chr16-668 (+205101), chr16-890 (+207296), chr16-1755 (+221342), chr16-547 (+221972), chr16-1357 (+260483), chr16-1055 (+306607), chr16-438 (+322882), chr16-799 (+370750), chr16-723 (+374370)
SOCS3	chr17-826 (+16249), chr17-1223 (+22384), chr17-51 (+30513), chr17-525 (+35276), chr17-1950 (+65135), chr17-2529 (+65997), chr17-2119 (+66730), chr17-2756 (+67237), chr17-1827 (+74770), chr17-2118 (+75749)
SP100	chr2-2369 (-3570), chr2-1251 (+19), chr2-4992 (+2390), chr2-4993 (+23702), chr2-190 (+41431), chr2-6135 (+162016), chr2-3944 (+173551), chr2-475 (+227527), chr2-1817 (+227979), chr2-319 (+244660), chr2-1121 (+252511), chr2-4996 (+253022), chr2-4193 (+262424), chr2-2680 (+284442)
STAT1	chr2-3280 (-100570), chr2-4931 (-37861), chr2-4508 (-24304), chr2-3911 (-6895), chr2-1929 (+17051), chr2-841 (+43193), chr2-2932 (+52159), chr2-3279 (+66201), chr2-3910 (+122614)
STAT2	chr12-2875 (+1157)
TRIM56	chr7-1633 (+14780), chr7-341 (+22883)
TYK2	chr19-577 (+7643)
USP18	chr22-9 (-35843), chr22-503 (-30016)
XAF1	chr17-341 (-3177), chr17-774 (-2667), chr17-3083 (+40776)

Supplementary Table 5: Specific genes and genomic region of peaks driving the associations of the ChIPseq dataset of SMAD1-bound loci from BMP4-treated U937 cells with type I interferon associated pathways (see Supplementary Figure 3c).

GO BP: Regulation of type I IFN-mediated signalling pathway	
Genes	**Genomic regions of peaks**
HSP90AB1	chr6-102 (-21152), chr6-1128 (+399)
IFNAR1	chr21-140 (-75319), chr21-73 (-58374), chr21-141 (-19899), chr21-9 (+43342), chr21-199 (+55174), chr21-28 (+61679)
IFNAR2	chr21-194 (-30994), chr21-72 (-17608), chr21-195 (-88), chr21-140 (+19664), chr21-73 (+36609), chr21-141 (+75084)
JAK1	chr1-336 (-55453), chr1-1948 (+73460), chr1-1947 (+81652), chr1-35 (+102205)
MAVS	chr20-323 (-7251), chr20-325 (-3104), chr20-259 (+31988)
NLRC5	chr16-109 (+48152)
PTPN1	chr20-170 (-312648), chr20-6 (-217614), chr20-32 (-211571), chr20-428 (-191478), chr20-222 (-162049), chr20-39 (-123715), chr20-223 (-122992), chr20-289 (-115560), chr20-224 (-69308), chr20-116 (-54498), chr20-225 (+7615), chr20-290 (+31525), chr20-171 (+48534), chr20-291 (+132192), chr20-431 (+156602), chr20-4 (+181096)
PTPN11	chr12-355 (-4770), chr12-767 (+347)
PTPN6	chr12-385 (+14306), chr12-274 (+18670)
SOCS1	chr16-162 (+407), chr16-105 (+22839), chr16-454 (+54144), chr16-161 (+95372), chr16-46 (+150939), chr16-65 (+283229), chr16-17 (+283764), chr16-160 (+311713), chr16-21 (+369046)
SOCS3	chr17-198 (+48), chr17-163 (+44103), chr17-16 (+87691), chr17-534 (+88138), chr17-80 (+96677), chr17-79 (+101317), chr17-372 (+109018)
STAT1	chr2-488 (-6284), chr2-847 (-32)
STAT2	chr12-654 (+165)

GO BP: type I IFN-mediated signalling pathway	
Genes	**Genomic regions of peaks**
ADAR	chr1-647 (-21086), chr1-2080 (-8907), chr1-2079 (+321), chr1-1464 (+14668)
EGR1	chr5-242 (-55)
GBP2	chr1-1062 (+4245)
HLA-A	chr6-191 (+22541), chr6-270 (+25244)
HLA-C	chr6-730 (-123929), chr6-1032 (-15655)
IFIT3	chr10-577 (+30635)
IFITM3	chr11-568 (-35465)
IFNAR1	chr21-140 (-75319), chr21-73 (-58374), chr21-141 (-19899), chr21-9 (+43342), chr21-199 (+55174), chr21-28 (+61679)
IFNAR2	chr21-194 (-30994), chr21-72 (-17608), chr21-195 (-88), chr21-140 (+19664), chr21-73 (+36609), chr21-141 (+75084)
IRF1	chr5-508 (-216), chr5-717 (+22925), chr5-716 (+53074), chr5-191 (+63993), chr5-29 (+67964)
IRF2	chr4-124 (+22616)
IRF4	chr6-246 (+213013), chr6-155 (+266736), chr6-885 (+272295)
JAK1	chr1-336 (-55453), chr1-1948 (+73460), chr1-1947 (+81652), chr1-35 (+102205)
PTPN1	chr20-170 (-312648), chr20-6 (-217614), chr20-32 (-211571), chr20-428 (-191478), chr20-222 (-162049), chr20-39 (-123715), chr20-223 (-122992), chr20-289 (-115560), chr20-224 (-69308), chr20-116 (-54498), chr20-225 (+7615), chr20-290 (+31525), chr20-171 (+48534), chr20-291 (+132192), chr20-431 (+156602), chr20-4 (+181096)
PTPN11	chr12-355 (-4770), chr12-767 (+347)
PTPN6	chr12-385 (+14306), chr12-274 (+18670)

SOCS1	chr16-162 (+407), chr16-105 (+22839), chr16-454 (+54144), chr16-161 (+95372), chr16-46 (+150939), chr16-65 (+283229), chr16-17 (+283764), chr16-160 (+311713), chr16-21 (+369046)
SOCS3	chr17-198 (+48), chr17-163 (+44103), chr17-16 (+87691), chr17-534 (+88138), chr17-80 (+96677), chr17-79 (+101317), chr17-372 (+109018)
SP100	chr2-511 (-17177), chr2-91 (+243208)
STAT1	chr2-488 (-6284), chr2-847 (-32)
STAT2	chr12-654 (+165)
XAF1	chr17-396 (-17078)

GO BP: response to type I IFN	
Genes	**Genomic regions of peaks**
ADAR	chr1-647 (-21086), chr1-2080 (-8907), chr1-2079 (+321), chr1-1464 (+14668)
EGR1	chr5-242 (-55)
GBP2	chr1-1062 (+4245)
HLA-A	chr6-191 (+22541), chr6-270 (+25244)
HLA-C	chr6-730 (-123929), chr6-1032 (-15655)
IFIT3	chr10-577 (+30635)
IFITM3	chr11-568 (-35465)
IFNAR1	chr21-140 (-75319), chr21-73 (-58374), chr21-141 (-19899), chr21-9 (+43342), chr21-199 (+55174), chr21-28 (+61679)
IFNAR2	chr21-194 (-30994), chr21-72 (-17608), chr21-195 (-88), chr21-140 (+19664), chr21-73 (+36609), chr21-141 (+75084)
IRF1	chr5-508 (-216), chr5-717 (+22925), chr5-716 (+53074), chr5-191 (+63993), chr5-29 (+67964)
IRF2	chr4-124 (+22616)
IRF4	chr6-246 (+213013), chr6-155 (+266736), chr6-885 (+272295)
JAK1	chr1-336 (-55453), chr1-1948 (+73460), chr1-1947 (+81652), chr1-35 (+102205)
PTPN1	chr20-170 (-312648), chr20-6 (-217614), chr20-32 (-211571), chr20-428 (-191478), chr20-222 (-162049), chr20-39 (-123715), chr20-223 (-122992), chr20-289 (-115560), chr20-224 (-69308), chr20-116 (-54498), chr20-225 (+7615), chr20-290 (+31525), chr20-171 (+48534), chr20-291 (+132192), chr20-431 (+156602), chr20-4 (+181096)
PTPN11	chr12-355 (-4770), chr12-767 (+347)
PTPN6	chr12-385 (+14306), chr12-274 (+18670)
SOCS1	chr16-162 (+407), chr16-105 (+22839), chr16-454 (+54144), chr16-161 (+95372), chr16-46 (+150939), chr16-65 (+283229), chr16-17 (+283764), chr16-160 (+311713), chr16-21 (+369046)
SOCS3	chr17-198 (+48), chr17-163 (+44103), chr17-16 (+87691), chr17-534 (+88138), chr17-80 (+96677), chr17-79 (+101317), chr17-372 (+109018)
SP100	chr2-511 (-17177), chr2-91 (+243208)
STAT1	chr2-488 (-6284), chr2-847 (-32)
STAT2	chr12-654 (+165)
XAF1	chr17-396 (-17078)

Supplementary Table 6: Specific genes and genomic region of peaks driving the associations of the ChIPseq dataset of SMAD1-bound loci from BMP4-treated K562 cells with Type I interferon associated pathways (see Supplementary Figure 3d).

Supplementary Figure 1

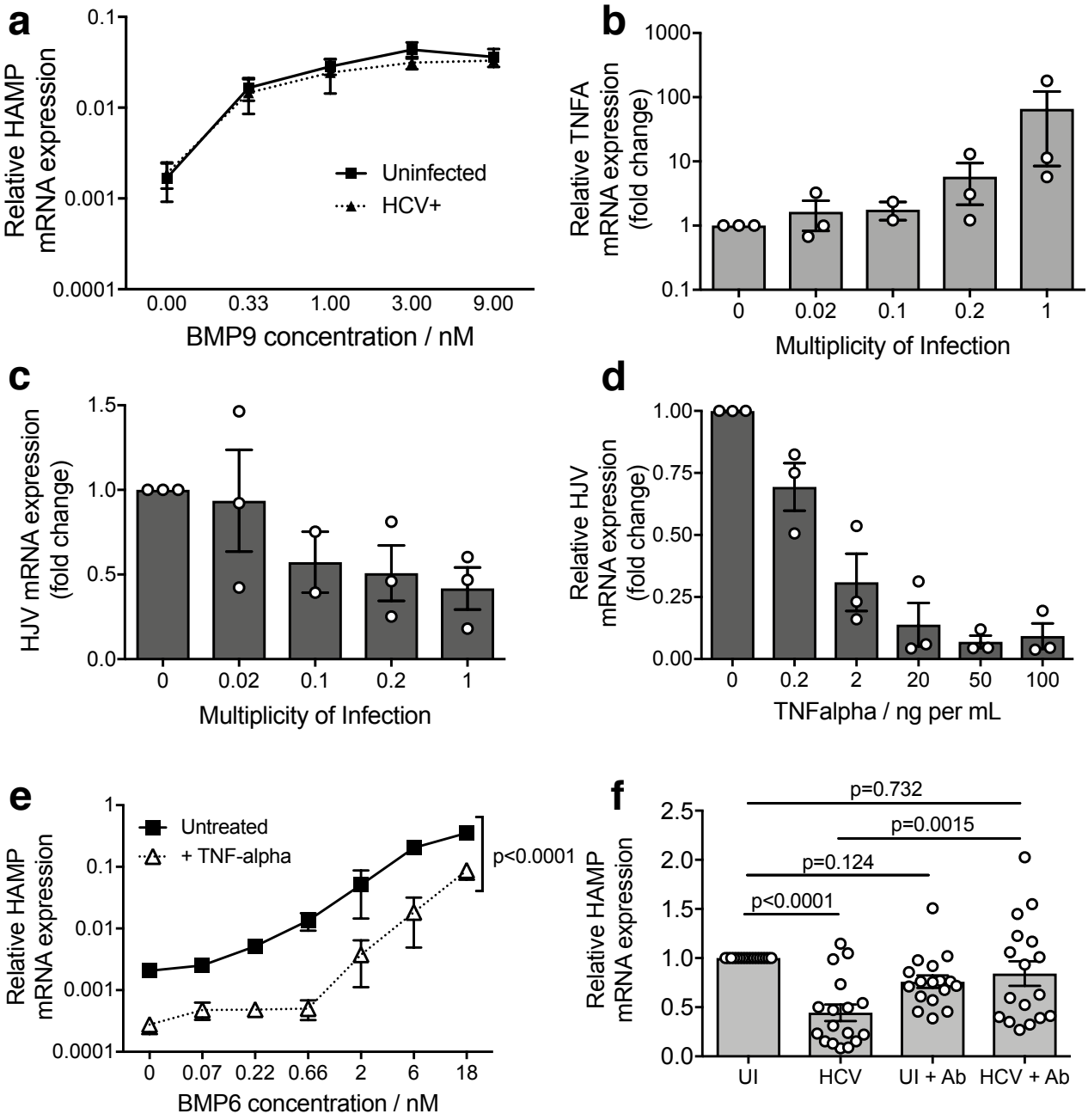

Supplementary Figure 1: Reduced upregulation of hepcidin in response to BMP6 in HCV infected cells is likely via TNFa induction

a Uninfected or HCV-infected (MOI = 0.02) Huh7.5 cells were incubated with a titration of BMP9 overnight; *HAMP* mRNA induction in response to BMP9 was not suppressed in HCV-infected cells (two-tailed Wilcoxon matched pairs test; p=0.2293; n=3 biologically independent experiments). **b** *TNFA* mRNA levels increased with multiplicity of infection (n=3 biologically independent experiments; plots depict mean +/- SEM expression relative to the endogenous control gene *GAPDH*, compared to untreated cells). **c** *HJV* mRNA levels, quantified by qRT-PCR relative to GAPDH expression, declined in HCV-infected Huh7.5 cells with increasing multiplicities of infection (MOI) (n=3 biologically independent experiments; plots depict mean +/- SEM expression relative to *GAPDH*, compared to uninfected cells). **d** Incubation of Hep3B cells with exogenous TNF alpha results in the loss of *HJV* mRNA expression (n=3 biologically independent experiments; plots depict mean +/- SEM expression relative to *GAPDH*, compared to untreated cells). **e** Pre-treatment of Hep3B cells with 20ng/mL TNF-alpha for 48h reduced their response to overnight incubation with BMP6 (two-tailed Wilcoxon matched pairs test; n=3 biologically independent experiments).
f Neutralizing anti-TNF-alpha antibody (Ab, 0.2 ug/mL) over the course of a 10-day HCV infection (MOI=0.02) restored BMP-mediated hepcidin (*HAMP*) induction. Data are from n=3 biologically independent experiments, each containing a titration of 5-6 BMP6 concentrations ranging from 0.22 – 18nM: data are normalized to the *HAMP* expression level in uninfected (UI) cells given the equivalent BMP6 dose; graphs depict mean relative expression +/- SEM; Repeated measures one-way ANOVA with Bonferroni's multiple comparison test adjusted p-values shown.

Supplementary Figure 2

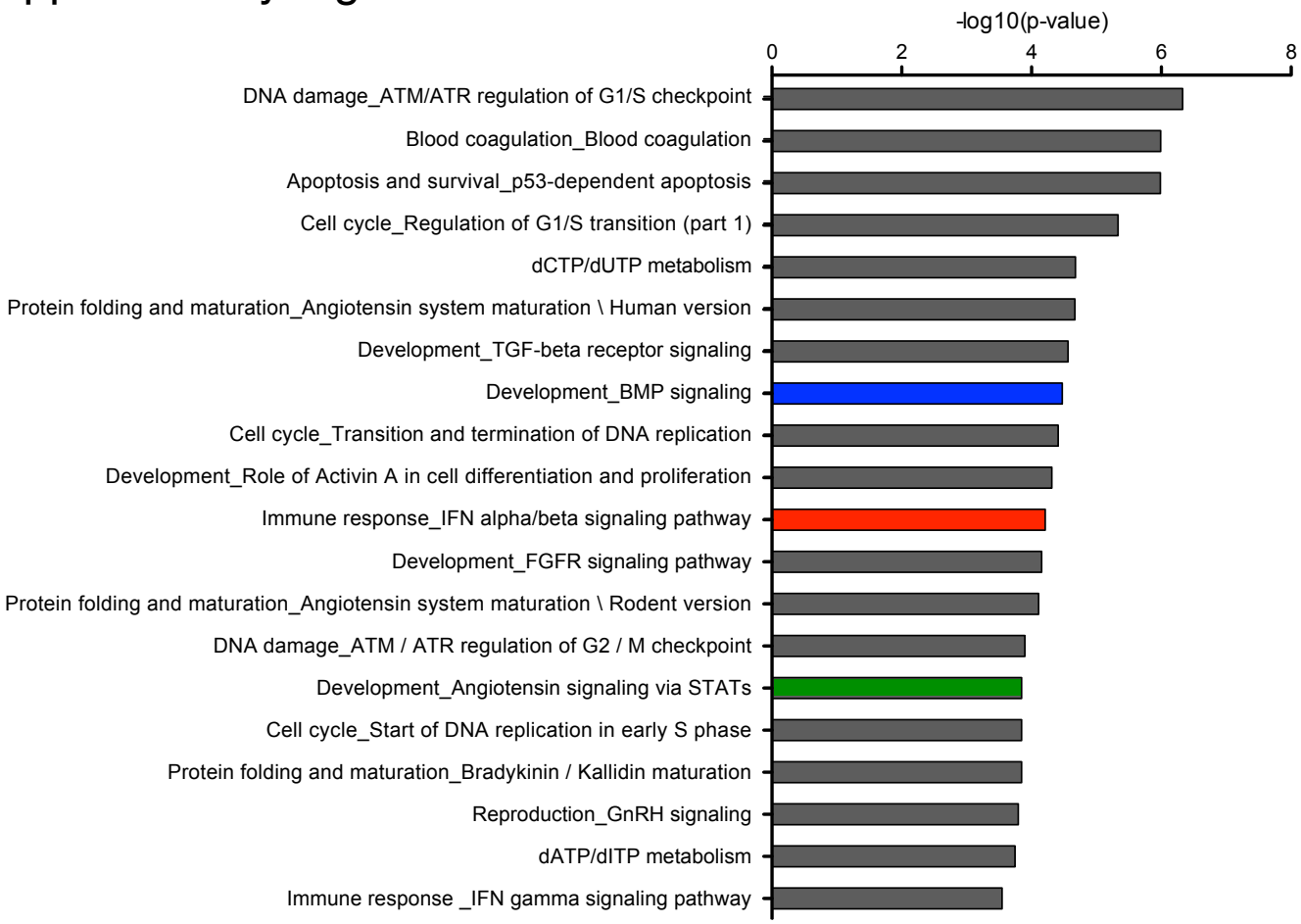

Supplementary Figure 2: BMP6 induces a transcriptome reminiscent of Type I IFN signaling

Pathway analysis of microarray from Huh7.5 cells treated with 18nM BMP6 for 24 hours, compared to vehicle treated cells (n = 2 independent experiments, each run in triplicate, giving a total of 6 RNA extracts per condition). The top 20 ‘pathway maps’ were raised by MetaCore software analysis of the transcriptome of BMP6 treated Huh7.5 cells. The blue bar highlights the BMP signaling pathway, the red bar highlights the Type I IFN signaling pathway, the green bar highlights development/ angiotensin signaling mediated by STAT, all are significant. P-values represent results of the hypergeometric test, identical to the corresponding one-tailed version of Fisher's exact test, as implemented by Metacore; FDR was set at 0.05.

Supplementary Figure 3

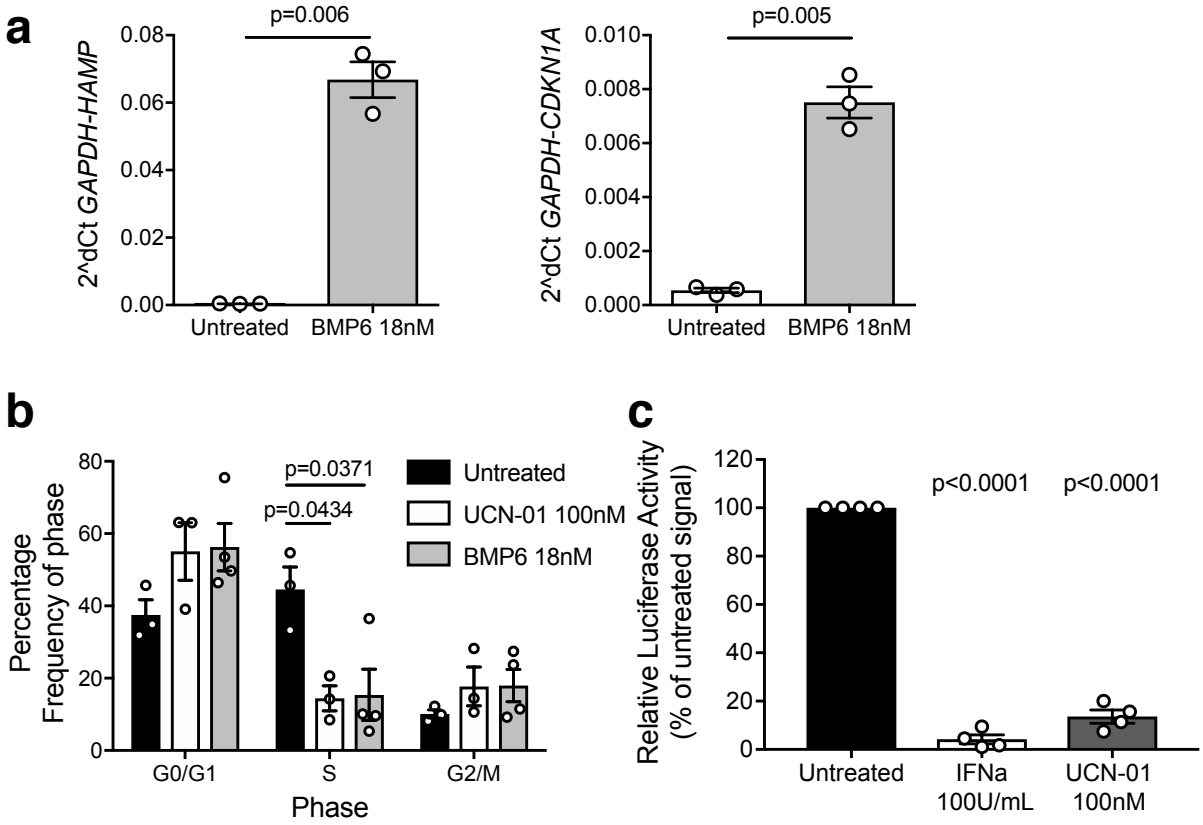

Supplementary Figure 3: BMP6, cell-cycle progression and HCV replication.
a Huh7 cells were incubated with BMP6 18 nM for 24 h, followed by qRT-PCR analysis of HAMP, encoding the established BMP-target gene hepcidin and CDKN1A (encoding p21) mRNA expression relative to the endogenous control gene GAPDH**.** Plots display mean ± SEM; two-tailed paired t tests based on n=3 biologically independent experiments in duplicate wells.
b Huh7 cells were untreated or incubated with the cytostatic agent UCN-01 or recombinant human BMP6 for 48h, followed by 30 minutes pulsed incorporation of BrdU. Cells were harvested and immunostained for incorporated BrdU and exposed to the DNA-intercalating dye propidium iodide. Percentages of cells in each phase of the cell cycle were then quantified by two-colour flow-cytometry. Incubation with BMP6 promotes a shift in phase frequencies akin to that observed with the cytostatic drug UCN-01, characterized by a statistically-significant reduction in the percentage of cells in S-phase. Data from n=3 biologically independent experiments; plots depict mean +/- SEM; one-way ANOVA within each phase grouping: Bonferroni's multiple comparison test adjusted p-values shown.
c OR6 cells were incubated with recombinant human IFNα-2a or UCN-01 and assayed at 72 h post-incubation for Renilla luciferase activity (indicating HCV replicon activity). Data from n=3 biologically independent experiments conducted in triplicate wells; plots depict mean +/- SEM; repeated measures ANOVA: Bonferroni's multiple comparison test adjusted p-values with respect to untreated cells shown. UCN-01 does not directly inhibit the Renilla luciferase reporter enzyme expressed by OR6 cells (not shown).

Supplementary Figure 4 (legend overleaf)

a

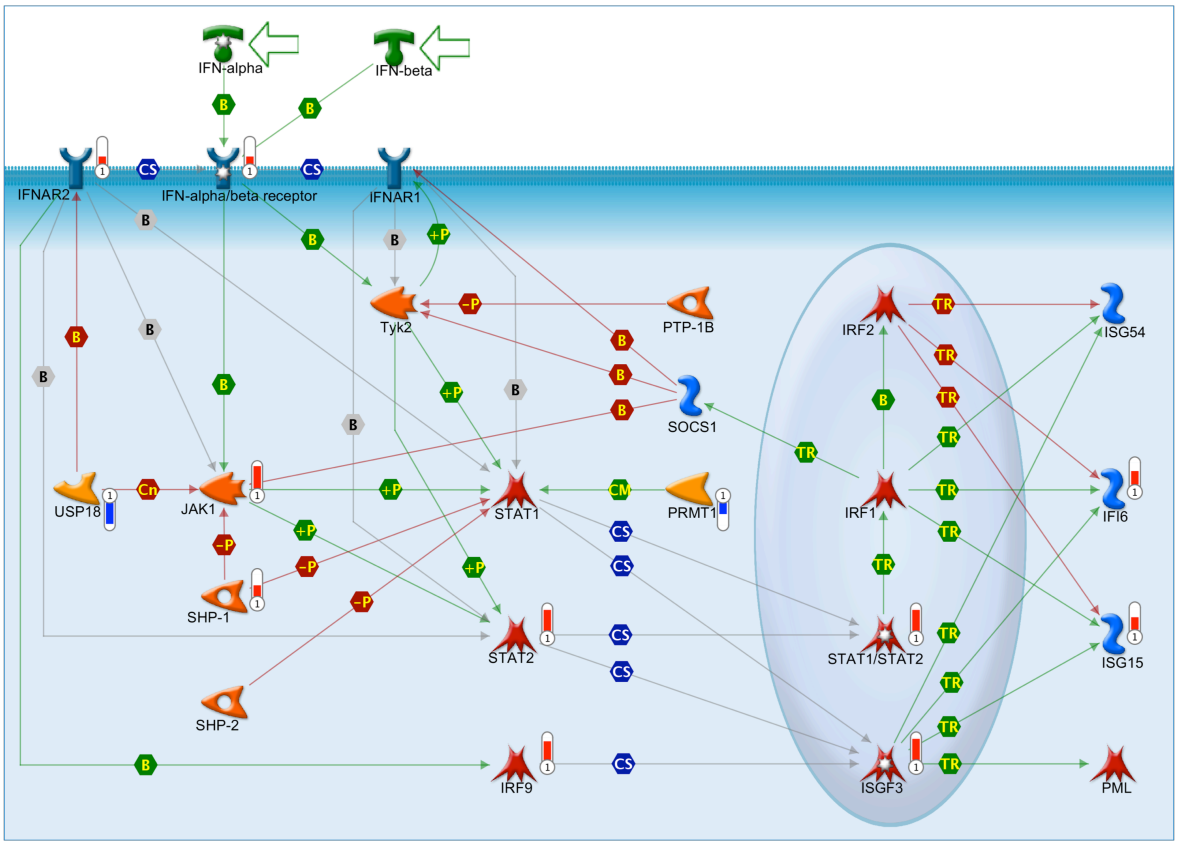

b

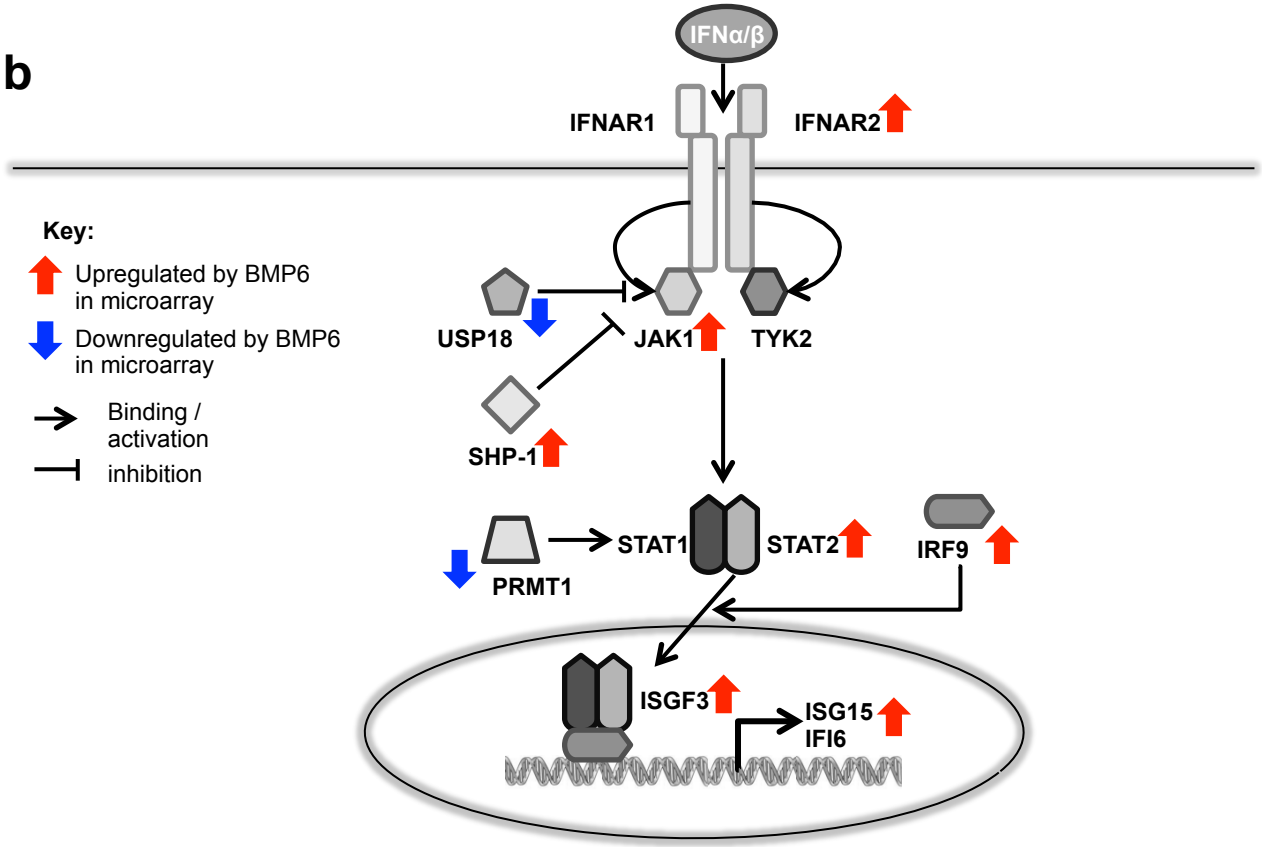

Supplementary Figure 4: BMP6-regulated IFN pathway–related genes in the Type I IFN signaling network

a Metacore output of the type I IFN signaling pathway with genes upregulated by BMP6 (IFNAR2, JAK1, STAT2, IRF9, ISG15, IFI6) indicated by red 'thermometer' symbol and genes downregulated by BMP6 (USP18, PRMT1) indicated by blue 'thermometer' signal. **b** Clarified scheme of IFN signaling pathway with upregulated by BMP6 (IFNAR2, JAK1, STAT2, IRF9, ISG15, IFI6) indicated by red up arrow and genes downregulated by BMP6 (USP18, PRMT1) indicated by blue down arrow.

Supplementary Figure 5

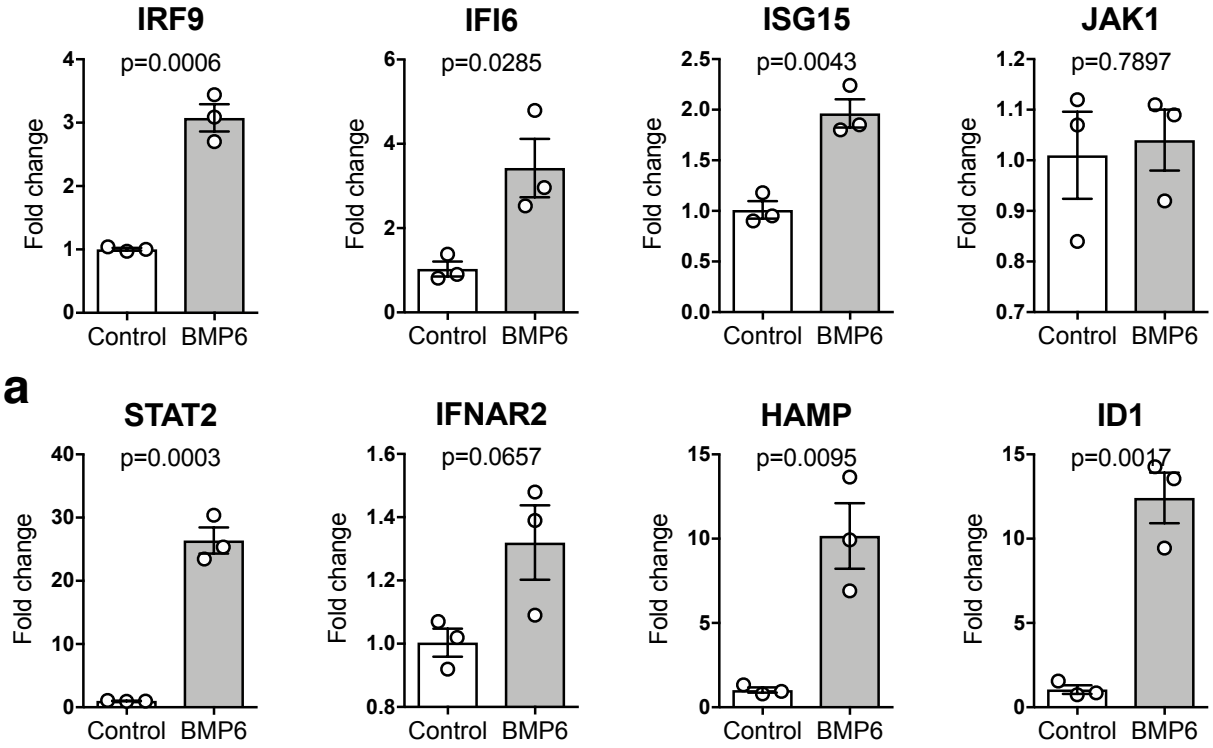

Supplementary Figure 5: mRNA expression of IFN-pathway related and BMP-pathway related genes in hepatocytes treated with BMP6

a The levels of *IFNAR2, JAK1, STAT2, IRF9, ISG15, IFI6*, *HAMP* and *ID1* mRNA in control and BMP6-treated primary human hepatocytes. Results are presented as mean ± SEM (n=3 technical replicates) of the fold change compared with PBS-treated cells. Statistical significance was assessed using two-tailed Student's *t* tests.

Supplementary Figure 6

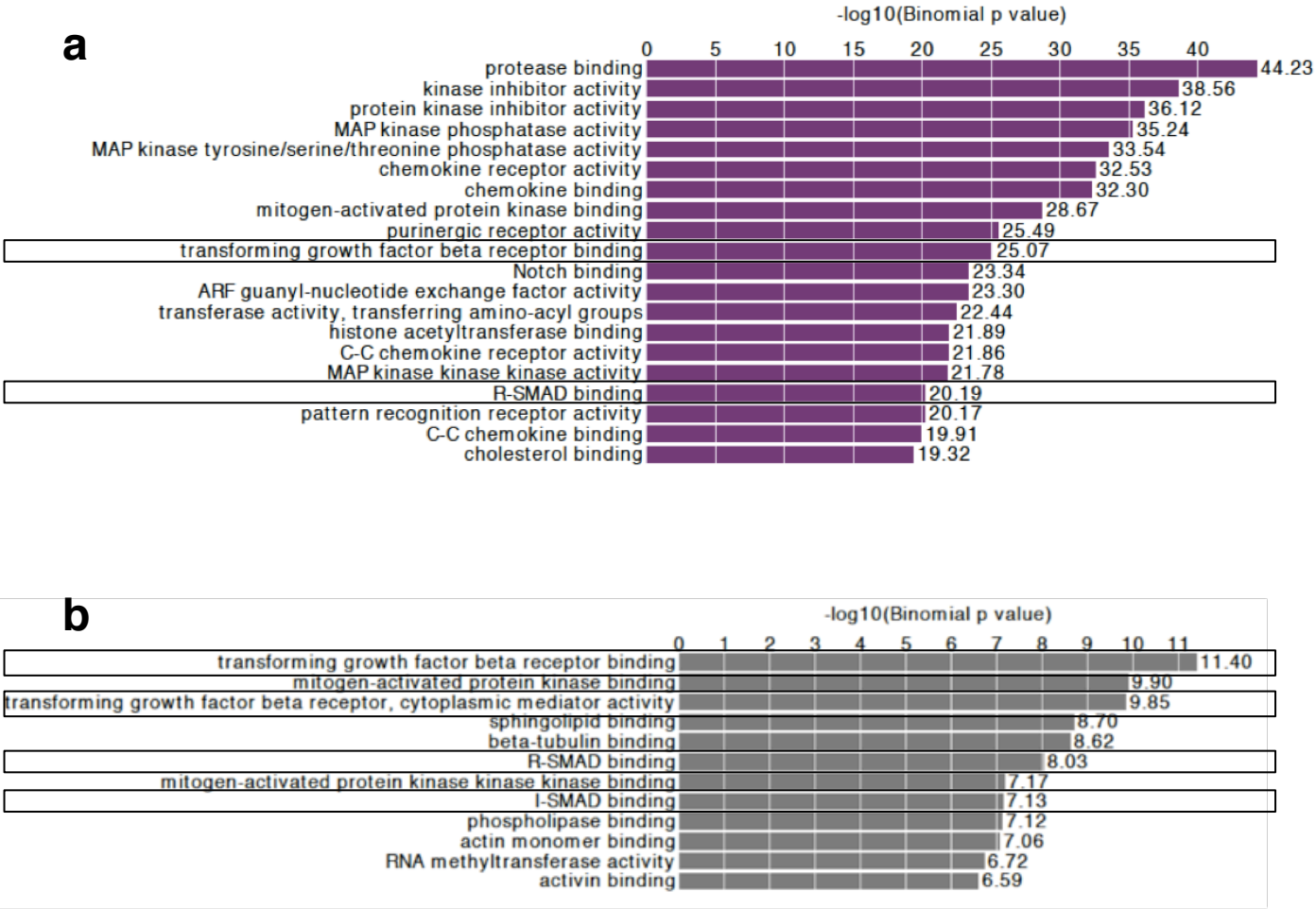

Supplementary Figure 6: Pathway analysis of SMAD1-bound loci in BMP4-treated U937 cells and K562 cells
GREAT Gene Set Enrichment Analysis (GSEA) for SMAD1 peaks derived from publicly available ChIPseq datasets for U937 cells (**a, c**) and K562 cells (**b, d**) treated with BMP4. Peaks identified with the Homer peak-calling algorithm were subjected to GSEA with the GREAT web-based tool. Pathways defined as significant by region-based binomial analysis with reference to the hg19 GRCh37 genome assembly were reported. GSEA results from interrogation of Gene Ontology (GO) Molecular Function (**a, b**) or Biological Process (**c, d**) databases are shown. For both cell types, Molecular Function databases report SMAD1-bound loci after BMP4 treatment were enriched in genes involved in TGF-beta / SMAD type signalling as expected (indicated by black boxes in **a, b**); and the Biological Processes databases report SMAD1-bound loci after BMP4 treatment were enriched in genes involved in the type I IFN response pathway (black boxes in **c, d**). Molecular Function and Biological Processes databases differ in their content of annotated pathways.

Supplementary Figure 6

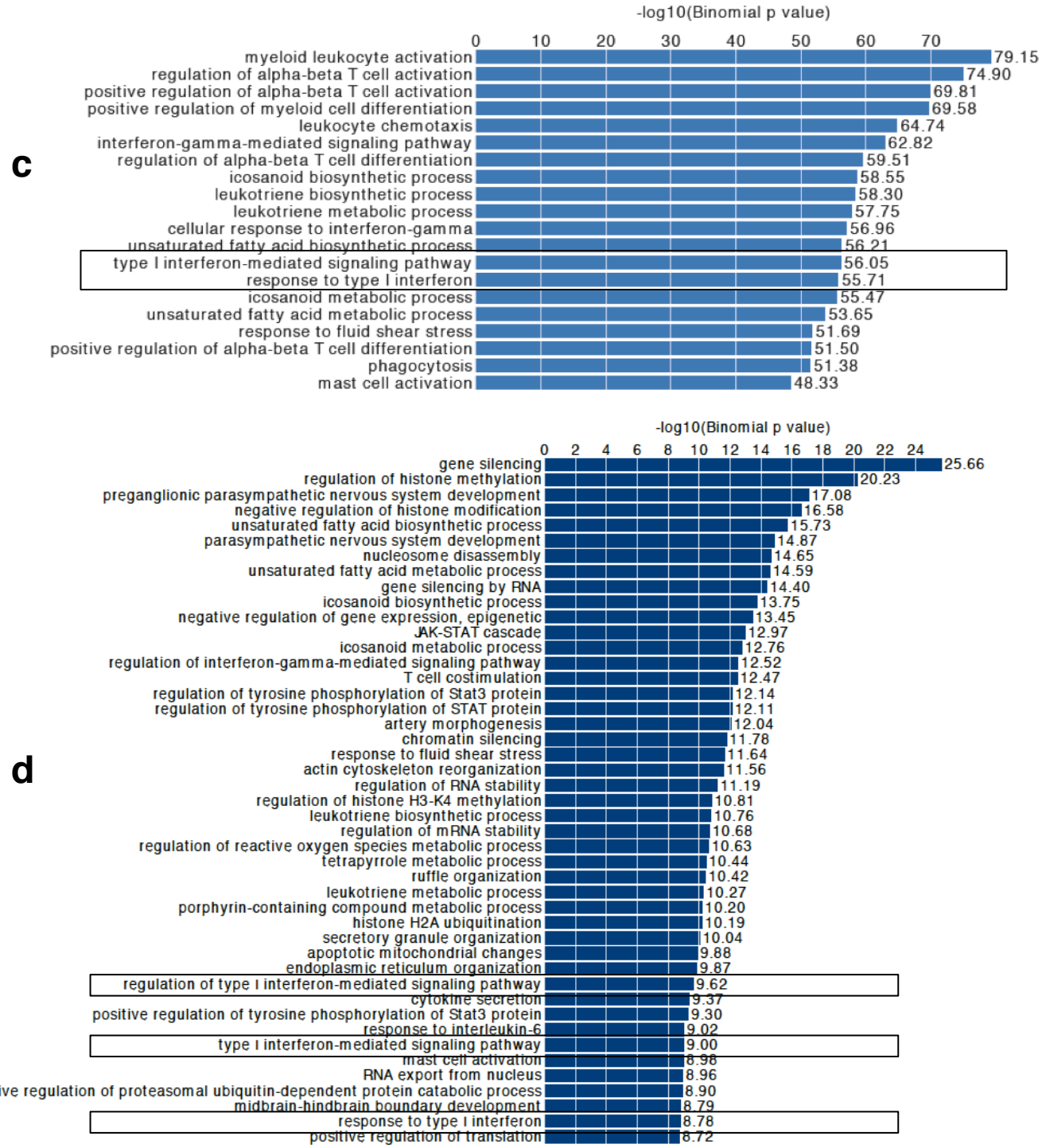

Supplementary Figure 6: Pathway analysis of SMAD1-bound loci in BMP4-treated U937 cells and K562 cells
GREAT Gene Set Enrichment Analysis (GSEA) for SMAD1 peaks derived from publicly available ChIPseq datasets for U937 cells (**a, c**) and K562 cells (**b, d**) treated with BMP4. Peaks identified with the Homer peak-calling algorithm were subjected to GSEA with the GREAT web-based tool. Pathways defined as significant by region-based binomial analysis with reference to the hg19 GRCh37 genome assembly were reported. GSEA results from interrogation of Gene Ontology (GO) Molecular Function (**a, b**) or Biological Process (**c, d**) databases are shown. For both cell types, Molecular Function databases report SMAD1-bound loci after BMP4 treatment were enriched in genes involved in TGF-beta / SMAD type signalling as expected (indicated by black boxes in **a, b**); and the Biological Processes databases report SMAD1-bound loci after BMP4 treatment were enriched in genes involved in the type I IFN response pathway (black boxes in **c, d**). Molecular Function and Biological Processes databases differ in their content of annotated pathways.

Supplementary Figure 7

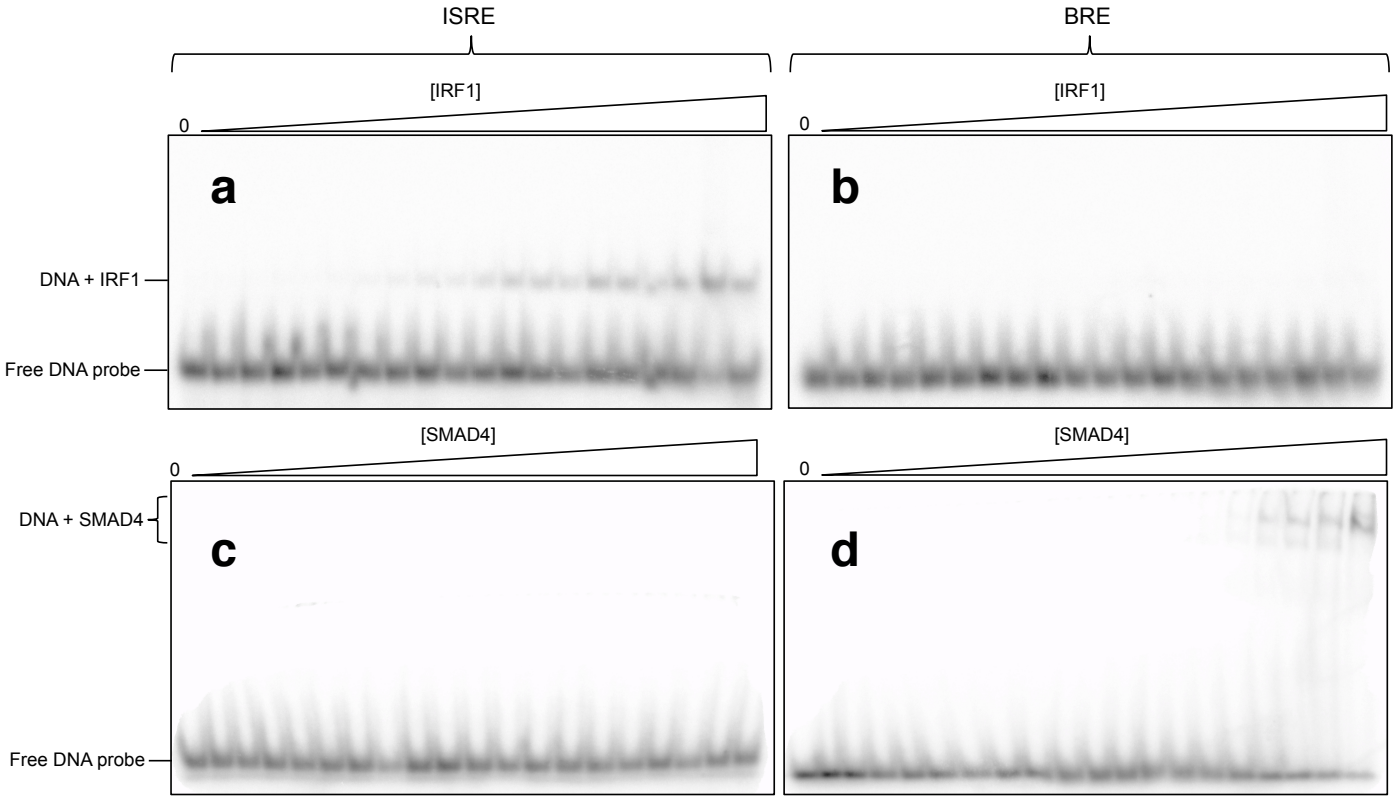

Supplementary Figure 7: EMSA of IRF1 binding ISRE and SMAD4 binding BRE
Electromobility shift assay of (a, b) IRF1 protein and (c, d) SMAD4 protein at two-fold serial dilutions from 0.5 µM incubated with 0.5 nM DNA probe of 25 bp dsDNA of interferon stimulated response element (ISRE, **a, c**) and BMP response element (BRE, **b, d**) at 37°C for 10 minutes before returning to ice, then run on 8% (**a, b**) or 6% (**c, d**) non-denaturing PAGE at 100 V for 3 h at 4°C in 0.5 x TBE. ISRE + 1RF1 binding (**a**) and SMAD4 + BRE binding (**d**) are indicated. Experiments were repeated twice for IRF1 and three times with SMAD4 with similar results.

Supplementary Figure 8

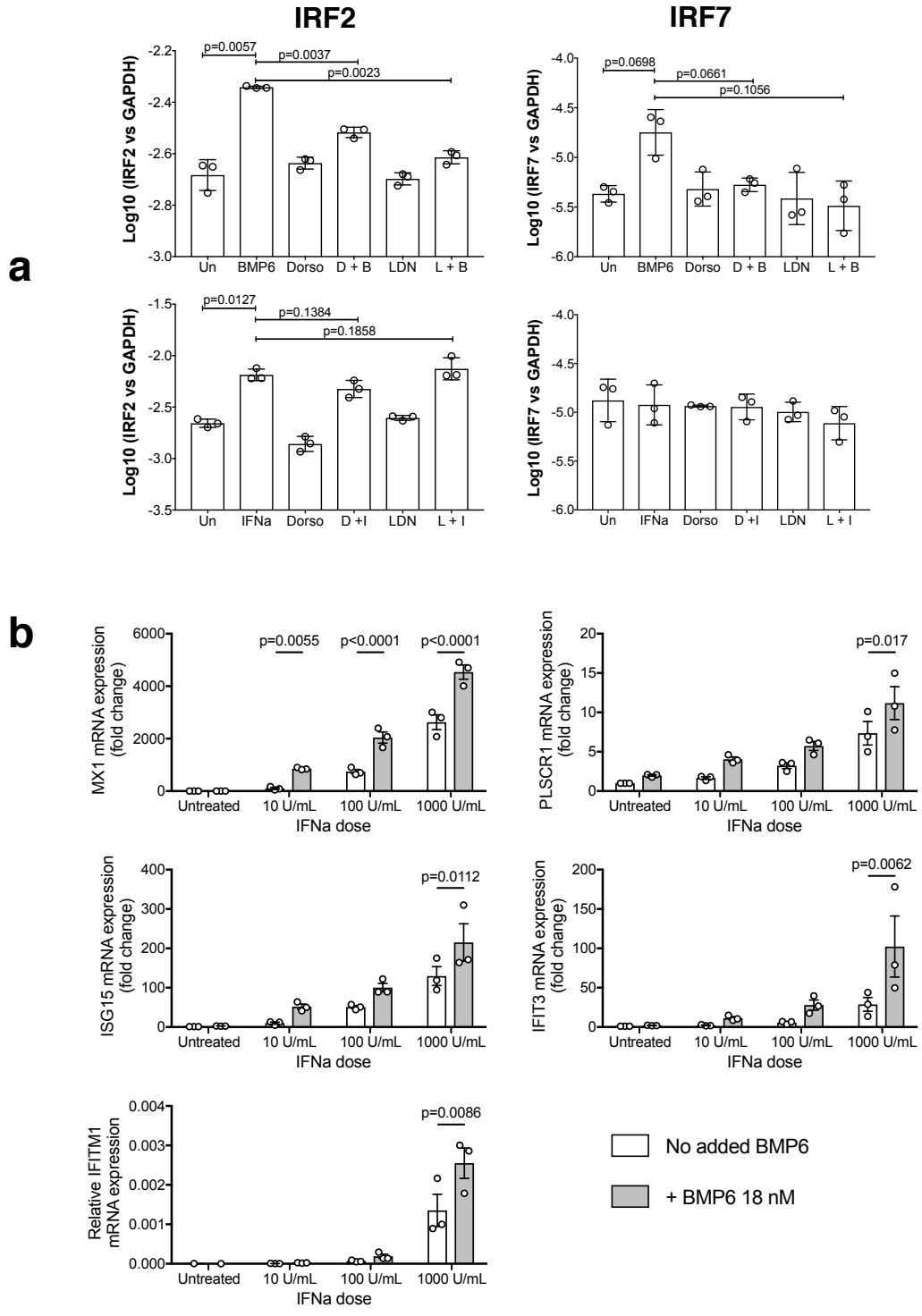

Supplementary Figure 8: BMP6 enhances expression of IRF2 and IRF7, and the IFN-alpha-mediated upregulation of IFN-stimulated genes

a The levels of *IRF2* and *IRF7* mRNA in Huh7.5 cells treated with 2uM dorsomorphin (Dorso) or 0.2uM LDN-193189 (LDN) 30 minutes prior to co-incubation with 18nM BMP6 for 20h (top row) or 1000U/mL IFN-alpha for 6h (bottom row). Plots display mean of log-transformed data ± SD; two-tailed paired t-tests on log-transformed data (n=3 independent biological replicates).
b *MX1*, *PLSCR1*, *ISG16*, *IFIT3*, and *IFITM1* mRNA expression in Huh7.5 cells treated with 18nM BMP6 followed immediately by co-incubation with a titration of IFN-alpha (10-1000U/mL) for 24h. Data from 3 biologically independent experiments are shown. Plots indicate means ± SEM; repeated measures ANOVA: Bonferroni's multiple comparison test adjusted p-values are indicated.

Supplementary Figure 9 (legend overleaf)

a

BMP4-SMAD1 K562

IFNa6h-IRF1 K562

BMP4-SMAD1 CD34+ erythrocyte

RSAD2 gene

H3K27ac active chromatin

H3K4Me1 enhancer-associated

H3K4Me3 promoter-associated

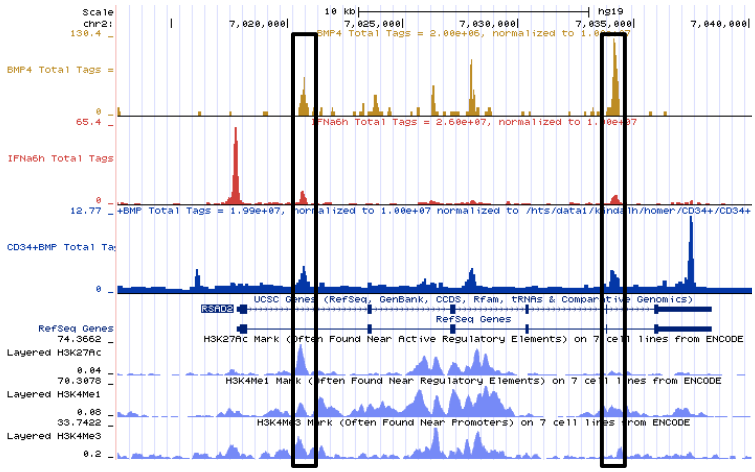

b

BMP4-SMAD1 K562

IFNa6h-IRF1 K562

BMP4-SMAD1 CD34+ erythrocyte

SSBP3 gene

H3K27ac active chromatin

H3K4Me1 enhancer-associated

H3K4Me3 promoter-associated

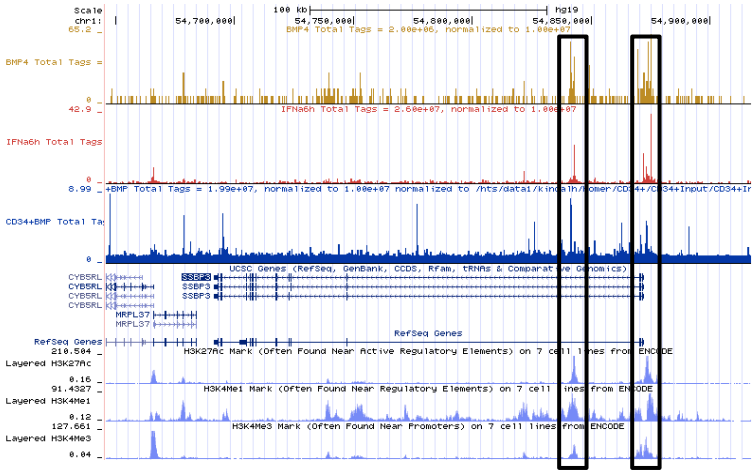

c

BMP4-SMAD1 K562

IFNa6h-IRF1 K562

BMP4-SMAD1 CD34+ erythrocyte

ZC3HAV1 gene

H3K27ac active chromatin

H3K4Me1 enhancer-associated

H3K4Me3 promoter-associated

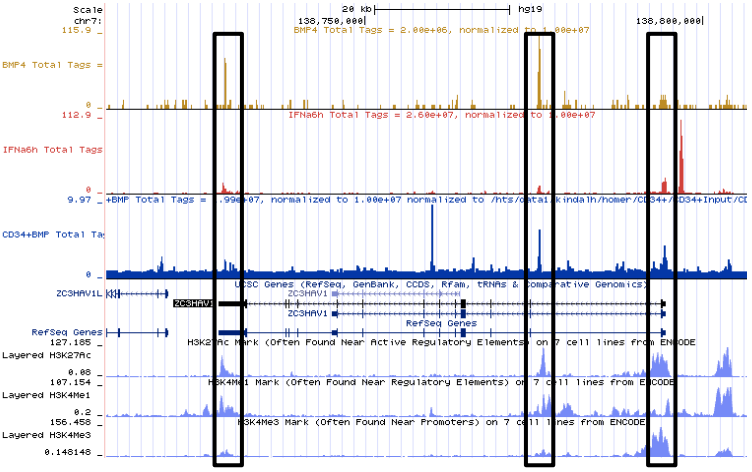

d

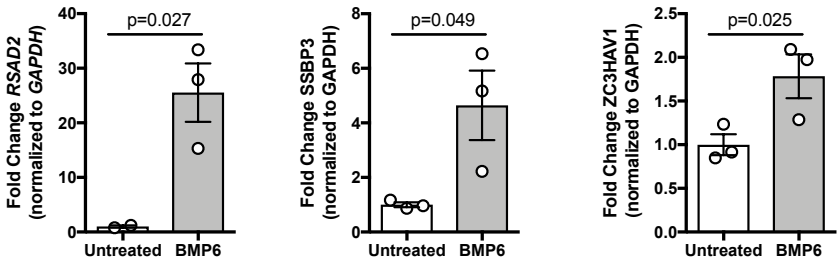

Supplementary Figure 9: SMAD1 and IRF1 ChIP peaks in similar active chromatin regions at RSAD2, SSBP3 and ZC3HAV1 loci

a-c Visualisation of gene loci showing: ChIP-seq for SMAD1 in BMP4-treated K562 cells, IRF1 in IFNα-treated K562 cells and SMAD1 in BMP4-treated CD34+ erythrocyte progenitors; gene structure, in accordance with RefSeq annotation (RefSeq/UCSC); ChIP-seq for histone marks H3K27ac, H3K4Me1 and H3K4Me3. Boxes denote instances of IRF1 and SMAD1 peak colocalisation in regions of active chromatin. Loci depicted are **a** *RSAD2* (encoding viperin) +/- 10kb, **b** *SSBP3* (encoding single-stranded DNA binding protein 3) +/-50kb, and **c** *ZC3HAV1* (encoding zinc finger antiviral protein-1) +/- 20kb.

d mRNA expression of *RSAD2, SSBP3* and *ZC3HAV1* was upregulated after incubation of Huh7.5 cells with 54nM BMP6 for 72h. Plots display mean fold change relative to untreated cells ± SEM; one-tailed paired t-tests (n=3 independent biological replicates).

Supplementary Figure 10 (legend overleaf)

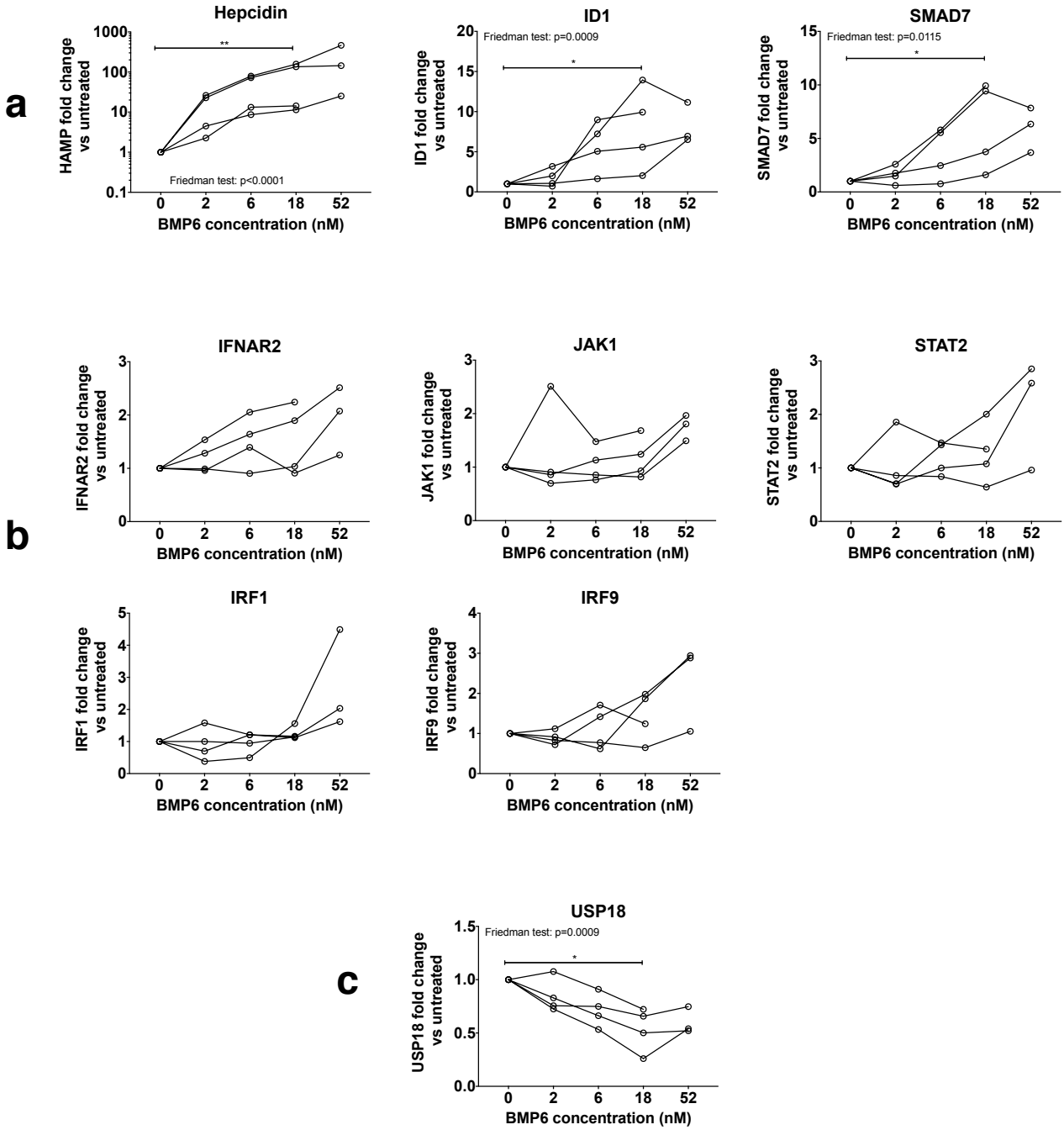

Supplementary Figure 10: Gene expression in HCV-infected Huh7.5 cells treated with BMP6

HCV infected Huh7.5 cells were incubated with a titration of BMP6 (2-52nM) for 5 days and then assayed for expression of

a the BMP6 target genes Hepcidin, ID1, and SMAD7

b five genes in the IFN signaling pathway (IFNAR2, JAK1, STAT2, IRF1, IRF9)

c the IFN pathway inhibitor USP18

Data summarise four biologically independent experiments. P-values report the results of Friedman tests (non-parametric repeated measures ANOVA) based on treatments 0, 2, 6 and 18nM BMP6 (52nM precluded owing to missing data from one of the four biological replicates); if not shown, Friedman test p-value >0.05; * or ** represents significance of specific comparisons with adjusted p-value <0.05 or <0.01 based on Dunn's multiple comparison post-test.

Supplementary Figure 11 (legend overleaf)

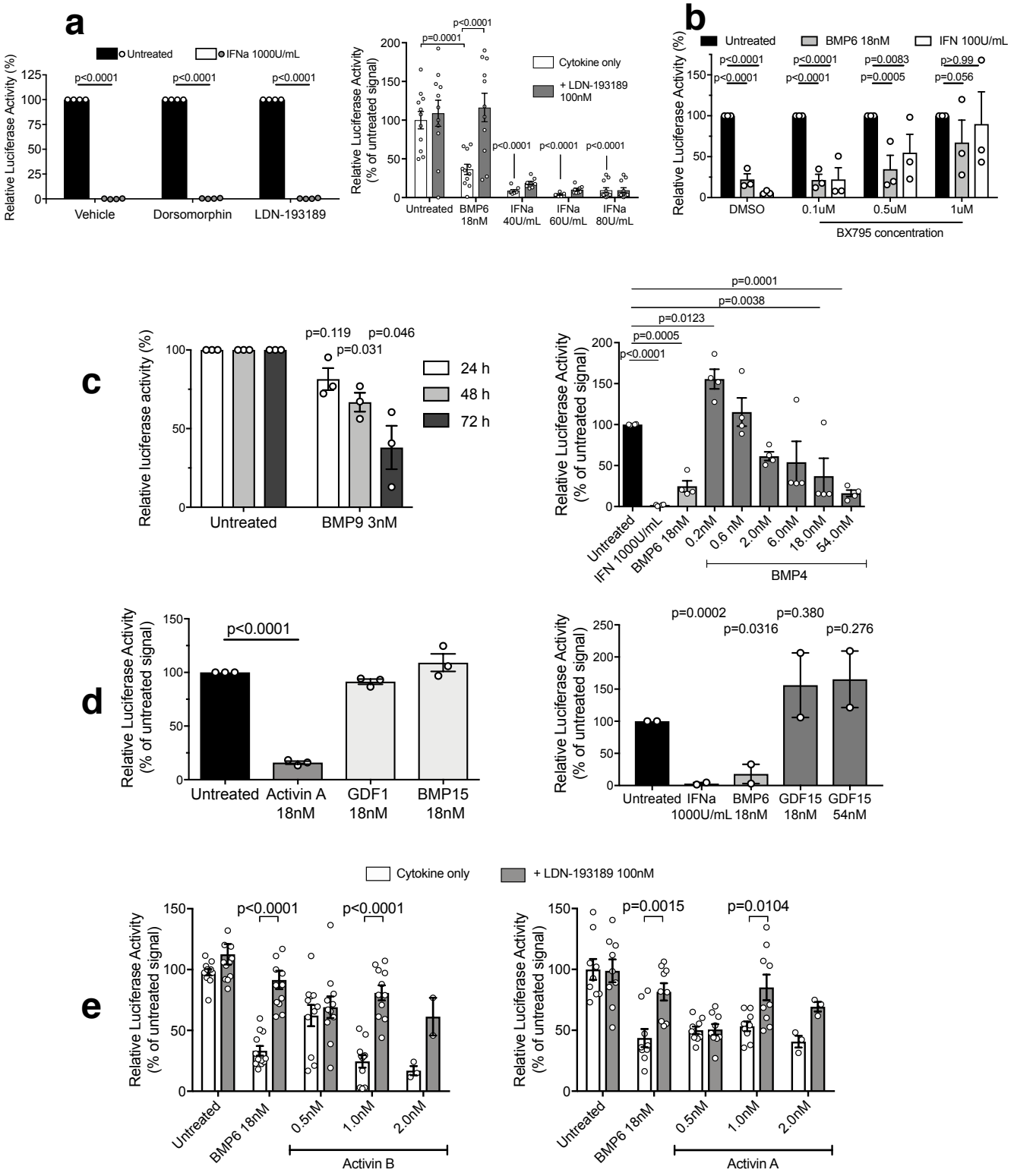

Supplementary Figure 11: Effect of BMP pathway inhibition, Bx795, BMPs and Activins on HCV replication

a Left - Luciferase activity in OR6 cells treated with 2uM dorsomorphin, 0.2uM LDN-193189 or vehicle control (water) for 30 minutes prior to co-incubation with 1000U/mL IFN-alpha for 24h (two tailed paired t-test; n=3 biologically independent experiments; plots depict mean +/- SEM); Right - Luciferase activity in OR6 cells treated with 100nM LDN-193189 or vehicle control (water) for 30 minutes prior to co-incubation with 18nM BMP6 or a titration of IFN-alpha (40, 60 80U/mL) for 72h. Data from n=3 experiments containing 3-5 replicates (fewer replicate experiments for IFNa 40 and 60U/mL were available); plots depict mean +/- SEM; one-way ANOVA: Bonferroni's multiple comparison test adjusted p-values compared to untreated are indicated, except where otherwise marked.

b OR6 cells were exposed to BMP6 or IFN in the presence of increasing doses of Bx795 (TBK1 / IKKepsilon inhibitor) or its vehicle DMSO. Data from n=3 biologically independent experiments; plots depict mean +/- SEM; 2-way ANOVA: Bonferroni's multiple comparison test adjusted p-values are indicated.

c Left - Timecourse of luciferase activity in OR6 cells treated with 3nM BMP9 for 24, 48, 72h (two-tailed paired t test at each timepoint compared to untreated, n=3 biologically independent experiments; plots depict means +/- SEM); Right - Luciferase activity in OR6 cells treated for 24 hours with IFN-alpha, BMP6 or a titration of BMP4. Data from n=2 biologically independent experiments performed in duplicate; plots depict mean an +/- SEM; one-way ANOVA: Bonferroni's multiple comparison test adjusted p-values compared to untreated are indicated.

d Left - Luciferase activity in OR6 cells treated with Activin A, GDF1, or BMP15, for 24 hours; data from n=3 biologically independent experiments, each performed in triplicate. Plots indicate means ± SEM; repeated measures ANOVA: Bonferroni's multiple comparison test adjusted p-values, comparing to untreated, are indicated. Right - Luciferase activity in OR6 cells treated with IFN-alpha, BMP6, or GDF15; data from n=2 biologically independent experiments; p-values represent result of two-tailed unpaired t-tests, comparing to untreated.

e Luciferase activity 72h post-addition in OR6 cells treated with 0.1uM LDN-193189 for 30 minutes prior to addition of 18nM BMP6 or a dose titration of Activin B or Activin A. Data from n=3 biologically independent experiments comprising multiple replicates (2.0nM Activin A / Activin B was included in n=1 experiment); plots depict means +/- SEM; two-way ANOVA with Bonferroni's multiple comparisons test conducted between respective +/- LDN-193189 conditions.

Supplementary Figure 12

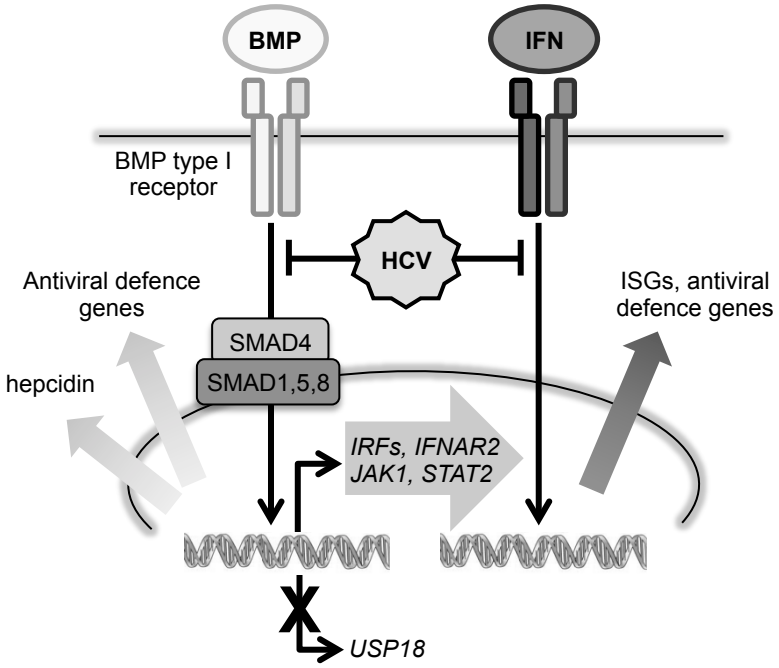

Supplementary Figure 12. Model of how BMP/SMAD signaling interacts with antiviral immunity and HCV infection. IFN activity and HCV infection are known to be mutually antagonistic; BMP/SMAD signaling is known to control iron homeostasis through regulating hepcidin. Our data show that BMP/SMAD signaling alters the expression of a gene repertoire (including downregulating USP18) leading to an enhancement of IFN activity, and has IFN-independent antiviral activity that suppresses HCV replication. Conversely, HCV inhibits BMP/SMAD signaling, suppressing hepcidin thereby predisposing to hepatic iron accumulation.

Supplementary Figure 13

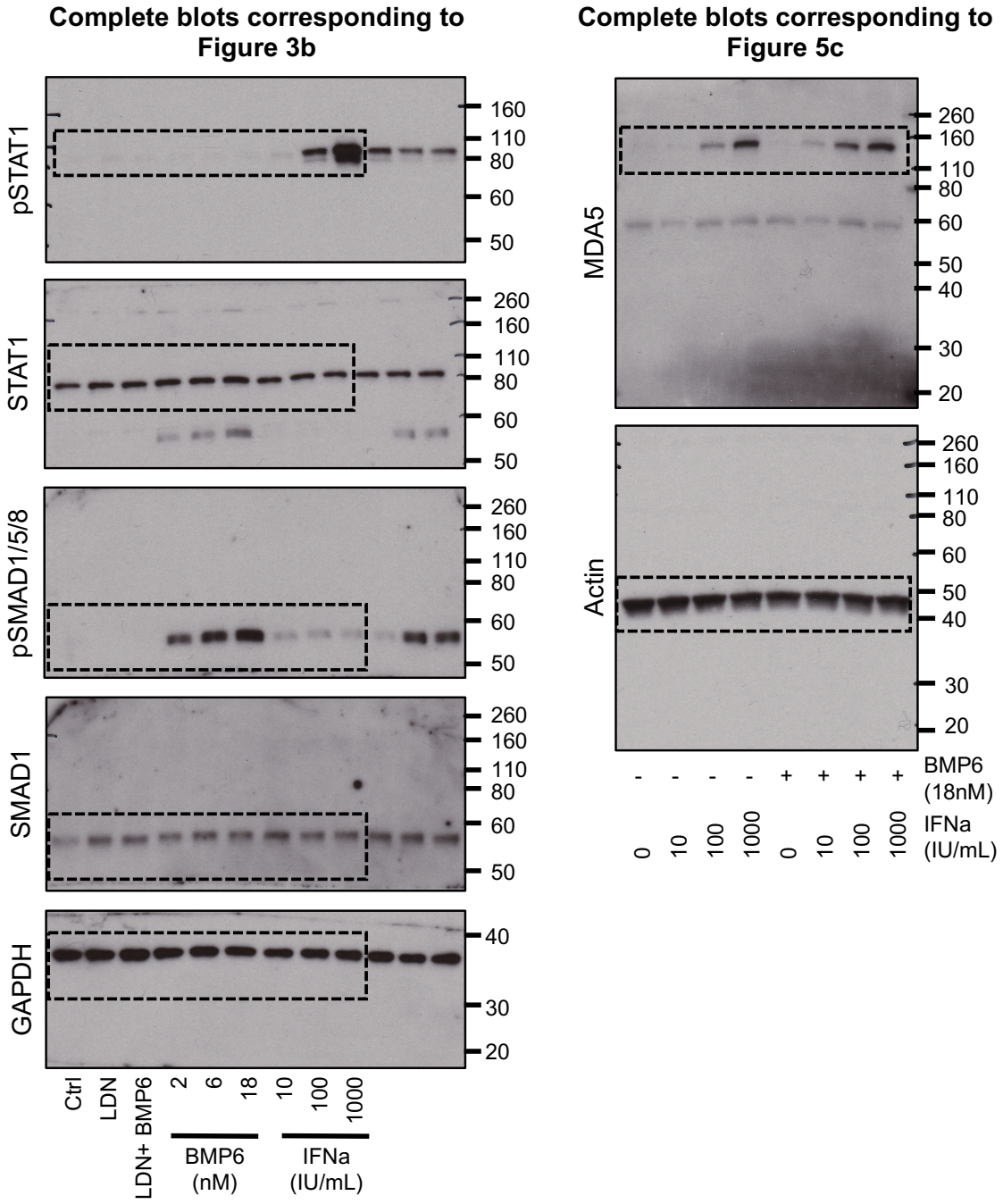

Supplementary Figure 13. Uncropped Western Blots. Full blots corresponding to the data shown in Figures 3b and 4c. Dashed lines indicate regions of blots shown in main figures. Molecular weight markers in kDa are indicated; LDN = LDN-193189.